Iraqi Journal for Computer Science and Mathematics

Journal Homepage: http://journal.esj.edu.iq/index.php/IJCM
e-ISSN: 2788-7421 p-ISSN: 2958-0544

The optimal scaling factor based on Secant Method for image watermarking using the hybrid DTCWT-DCT domain.

Mohamed Lebcir [1]*, Suryanti Awang [1,2], Ali Benziane [3]

[1] Faculty of Computing, Universiti Malaysia Pahang Al-Sultan Abdullah, 26600, Pekan, Pahang, Malaysia.

[2] Center of Excellence for Artificial Intelligence & Data Science, Universiti Malaysia Pahang Al-Sultan Abdullah, Lebuh Persiaran Tun Khalil Yaakob, 26300, Kuantan, Pahang, Malaysia.

[3] Faculty of Science and Technology, University of Djelfa, Algeria.

*Corresponding Author: Mohamed Lebcir

DOI: https://doi.org/10.52866/ijcsm.2024.05.01.017
Received Augest 2023 ; Accepted November 2023 ; Available online February 2024

ABSTRACT: This paper proposes an implementation of the secant optimization method on the watermark embedding in DTCWT domain. An objective function combining PSNR and NC (The Normalized Correlation) values calculated for a set of common attacks is used in the optimization process. The aim is to enhance the trade-off between robustness and imperceptibility against the various image processing attacks via an automatic and careful selection of the scaling factor using optimization. The watermark is inserted in the high energy bands of DCT-transformed sub-vectors, which were generated from the DTCWT coefficient decomposition of the host image. Experimental results performed on a set of 512×512 greyscale images, show better results than the existing schemes for most common image attacks such as compression, low-pass filtering and noise addition.

Keywords: Watermarking, DTCWT, DCT, Differential Method, Newton's Method, Secant Method, Scaling Factor.

1. INTRODUCTION

In recent years, it has become imperative for image watermarking technology for protecting copyrights to be robust against various types of attacks [1], [2]. Based on the domain of transform, the image watermarking techniques may be classified into spatial and frequency domains [3]. The direct image pixels' values are being used by the spatial domain the watermark embedding [4], although this domain is less complicated to be implemented [5], [6]. However, the spatial domain techniques are fragile against most image attacks [7], [8]. In the frequency domain, the watermark is inserted into the image transform coefficients; thus, it can embed more payloads and increase robustness against various attacks [8]. The transform domain's-based watermarking technologies have become more common for achieving strong image watermarking. Furthermore, combining two transform domains has the advantage that one of the two domains will compensate for the shortcomings of the other and provide robustness against a wider range of image attacks [9].

The watermark embedding system is affected by a conflict between imperceptibility and robustness as increasing the strength of embedding will decrease the visual quality of the watermarked image. So, to achieve the best trade-off between these two features, the usage of an optimal scaling factor is also crucial to achieve the optimal balance [10]. Several optimization methods are used to find the optimal scaling factor, but the determination of the ultimate solution by common optimization methods is considered difficult due to the multiple shortcomings every optimization algorithm endures [11]. With the advantages of the Secant (quasi-Newton) method, which proved to have higher accuracy and speed of convergence, it can achieve the best results when applied in the field of image watermarking.

Consequently, this paper proposes an optimized blind DTCWT-DCT scheme that can provide a strong balance between robustness and imperceptibility. Two DCT-transformed sub-vectors are generated from DTCWT's coefficients of the whole host image. After that, and based on the Secant method, the embedding scaling factor calculation is performed using only the high energy bands of the previous sub-vectors using a differential embedding manner. Meta-heuristic optimization, such as ant colony optimization (ACO), genetic algorithm (GA), and particle swarm optimization (PSO) are stochastic methods as they provide random solutions at each iteration; the best of the solutions is selected. Nevertheless, the low population variety as well as balancing between local optima are considered among the meta-heuristic methods shortcomings [12]. On the other hand, the Newton's optimization method that is based on a

numerical iterative approach can guarantees the convergence to the global optimum of the function if the initial guess is close enough to the optimum [11], [13]–[15]. Eventually, Newton's method will achieve higher accuracy and speed of convergence and, thus, achieve the best results when applied in the field of image watermarking. This will lead to tuning the watermark embedding using the optimized scaling factor for each host image which enables to withstand various image attacks and maintain the highest quality of watermarked image.

In the existing hybrid watermarking schemes based on DTCWT-DCT transform domain, the use of a hybrid domain can offer more robustness and security. However, one of the main drawbacks is the limited robustness of the watermark against some types of image processing attacks such as noise addition or geometric distortions in addition to the weak quality of the watermarked image which decrease the robustness-imperceptibility optimal balance. One of the keys to ensure optimal balance between robustness and imperceptibility is the determining the optimal scaling factors. To address these issues, this work proposes the Secant method to determine the optimal scaling factor in order to balance the demands of watermarking. Our contributions can be summarized as follows:

We propose an objective function by combining PSNR and NC functions with an amplification factor that put the PSNR and NC values in the same order. Next, maximizing the objective function shall maximize PSNR and NC functions. That is, we maximize the imperceptibility and the robustness at the same time. We use Secant method to maximize the objective function. This method is fast and has a super linear convergence rate. After the optimization, we use the optimal variable (the scaling factor) for the watermark embedding. Extensive tests on images were conducted by using optimal variable for watermarking on the images and we obtained plausible results of robustness and imperceptibility.

2. RELATED WORKS

The choice of the hybrid domain DTCWT-DCT domain has many advantages, it is able to improve the performance of robustness and imperceptibility in image watermarking schemes whereby the properties of the DTCWT domain are able to strongly deal with geometric attacks [16], and the properties of the DCT domain in the middle sub-band frequencies are able to withstand noise and compression attacks [13].

Several robust watermarking schemes have been proposed that utilize a hybrid domain of DTCWT and DCT. The scheme proposed by Ramani et al. (2010) aimed to protect the copyright of digital images through a combination of DTCWT and DCT domains. In this scheme, the watermark is embedded solely in the real parts of the DTCWT wavelet coefficients. If an unauthorized intruder attempts to extract the watermark, the watermarked image will not be distorted because the real part contains minimal information. The imaginary part of a watermark contains more significant data, making it easier to detect any alteration in the visual watermarked image if an attack occurs. Furthermore, the scaling factor used to achieve both invisibility and robustness in watermark embedding was only determined experimentally, whereas an adaptive scaling factor would be preferred to achieve a better trade-off between the two.

Bousnina et al. (2019) proposed another watermarking technique for fingerprint images which as well used a combination of DTCWT and DCT domains. In their scheme, the watermark was embedded in both the real and imaginary parts of the DTCWT wavelet high-frequency sub-bands, and a correlation method was used for blind watermark extraction. This study aims to refine watermarking methodologies for fingerprint images that are composed of different angles along with keeping the minutiae positions unchanged. Embedding a watermark in the high-frequency DTCWT coefficients may achieve high imperceptibility, but it decreases the robustness of the watermark against several image attack types. The low-frequency sub-band contains the most significant image data which is more robust against the attacks as it holds most of the image energy. Moreover, achieving a trade-off between robustness and imperceptibility requires an automatic adjustment of the insertion scaling factor during the embedding process which was used experimentally in their scheme.

Other works by Liu et al., Liu, Li, Cheng, et al., Liu, Li, Ma, et al. and Liu, Li, Zhang, et al. are considered recent related works that implemented the DTCWT-DCT under medical images. In these schemes, watermarks were embedded within low frequency coefficients using encryption technology to strengthen the security of the embedded watermark based on the Lorenz three dimensional hyperchaotic system, chaotic map and henon map respectively [17]–[20]. Their studies attempted to improve the security of the watermark's information using different encryption technologies. However, it is preferred using an optimized scaling factor during the embedding process which is a key factor in balancing between robustness and imperceptibility.

Other watermarking schemes based on a single transform such as DWT (Yadav et al., 2015) or DCT (Ariatmanto et al., 2020a; Ernawan et al., 2018), offered adaptability by using a robust adaptable factor with the image quality level, but they could demonstrate weakness against certain types of attacks such as cropping and noise addition. For instance, block-based scaling is a common issue with DCT watermarking that leads to failures against some image attacks. The directional selectivity of the DWT for diagonal features is also poor which decreases resistance against geometric attacks. Combining two domains offers the advantage of compensating for each domain's shortcomings which provides more robustness against a wider range of image attacks.

Researchers Mehta et al. (2016) and Tagesse et al. (2018) proposed watermarking schemes based on a single domain using SVD and DCT transforms respectively. Both schemes use GA to obtain the optimal scaling factor to be used in the embedding process in order to achieve a decent balance between robustness and imperceptibility against

some types of image attacks, but not against noise addition. The use of a threshold value for changing SVD coefficients may be inappropriate for various chosen blocks, and the poor directional selectivity of DWT for diagonal features may lead to failures against some image attacks. Combining the two domains can improve the robustness against a wider range of image attacks and provide a variety of requirements for embedding watermarks which would significantly improve the performance.

Another watermarking scheme used a combination of hybrid domain and optimization methods to guarantee the best possible trade-off between perceptual quality and robustness. Kang et al., proposed an image watermarking scheme that uses a hybrid domain DWT-DCT-SVD transform and an optimization method called PSO to obtain the embedding strength of the watermark adaptively based on the level of quality of the host image [21]. Their scheme was robust against most image processing attacks.

Proposed another scheme that combines the Bat Optimization Algorithm (BOA) with the Stationary Wavelet Transform (SWT) to improve the embedding strength [20]. Their proposed scheme showed a good balance between the quality of the watermarked image and the robustness of the watermark against various image attacks.

Other proposed watermarking schemes that are based on the hybrid transform DWT-SVD have been developed using optimization algorithms such as the dragonfly optimization algorithm (DOA), Particle Swarm Optimization (PSO), and Self-Adaptive Step Firefly Algorithm (SASFA) to obtain the optimal scaling factor [10], [22], [23]. These schemes have shown good performance in terms of balancing robust embedding and high imperceptibility.

Another proposed scheme suggests a security watermarking scheme that combines SVD, Lifting Wavelet Transform (LWT), and the Artificial Bee Colony (ABC) algorithm to enhance the security of the embedded watermark [24]. It enhanced the security of the embedded watermark by encrypting it before the embedding operations and obtained the optimal scaling factors based on the ABC optimization method.

In recent years, various optimization algorithms have been suggested to find the optimal amount of scaling factors including genetic algorithm (GA), differential evolution (DE), equilibrium optimization (EO), butterfly optimization algorithm (BOA), ant lion optimization (ALO), ant colony optimization (ACO), Artificial Bee Colony (ABC), Firefly Algorithm (FA), Particle Swarm Optimization (PSO), and Newton's method [11], [13]–[15], [25]–[32]. However, finding the optimal scaling factors by common optimization methods is considered difficult due to the multiple shortcomings every optimization algorithm endures[11]. Whereas methods such as Particle Swarm Optimization (PSO) and Ant Colony Optimization (ACO) are considered stochastic methods that provide random solutions at each iteration and the best of the solutions is selected. The algorithm of these methods is random in nature, which means that it uses stochastic optimization in some way. Therefore, the solution is based on the set of produced random variables and then choosing the best solution from those random solutions. The process would lead to finding a good solution but not the perfect possible solution. Thus, the effectiveness of those algorithms in finding the optimal solution is not guaranteed due to their random nature. Moreover, several stochastic methods have parameters that require careful tuning in order to achieve optimal performance. Determining the ideal values for these parameters could also present a difficult task [33], [34]. However, there is an optimization method known as Newton's method which is based on a numerical iterative approach that allows us to approach a solution at each iteration, which means that the process is then iterated using the new approximation as the starting point until a desired level of accuracy is reached [35]. Newton's method has been extensively studied and modified to improve the speed of convergence rate to the desired answer along with improving the accuracy of the approximate solutions [11], [13]–[15].

The quasi-Newton method - Secant method's advantages make it demonstrate better overall performance than Newton's method. Those advantages will be discussed in detail in the secant method section. This method could be utilized to find fast optimal solutions which makes it suitable for robust watermarking applications in reaching the optimal scaling factors.

3. THEORETICAL BACKGROUNDS

3.1 DUAL TREE COMPLEX WAVELET TRANSFORM (DTCWT)

The choice of the DTCWT domain has many advantages mainly because it is a better version of the wavelet transforms which has been reported to produce good results when used in image watermarking. In addition, its properties are used to preserve ridge angles, and it is able to strongly deal with geometric attacks where the watermark was embedded only in the real parts of the DTCWT wavelet coefficients [36].

The dual-tree complex wavelet transform allows the use of two actual DWTs. Hence, a joint transform is obtained from the two transforms where the real part is identified by the first DWT, and the imaginary part is identified by the second transform. In the DTCWT, 2-D wavelet function: W(a, b) = W(a)W(b) is integrated with the row-column of the wavelet transform, where W(a) is a complex wavelet represented by:

$$W(a) = W_r(a) + jW_i(a) \tag{1}$$

W(a, b) is obtained from the equation:

$$W(a,b) = [W_r(a) + jW_i(a)][W_r(b) + jW_i(b)]$$

$$= W_r(a)W_r(b) - W_i(a)W_i(b) + j[W_r(a)W_i(b) + W_i(a)W_r(b)] \quad (2)$$

The real part of the complex wavelet is taken, and then the sums of two separable wavelets are obtained:

$$\text{RealPart}\{ W_r(a,b) \} = W_r(a)W_r(b) - W_i(a)W_i(b) \quad \textbf{Error! No text of specified style in document.} \quad (3)$$

The pattern of the watermark looks like a checkerboard. Therefore, the watermarked image is subjected to the directional filter of the DTCWT for the purposes of decomposition. The output generated after one-directional filter from both low and high pass filters produced the subsequent images.

The real part is represented by the DTCWT coefficients obtained from the primary filter bank whereas the imaginary part is represented in the coefficients from the other filter. At each level of decomposition of the DTCWT wavelet, the coefficients of two complex (real and imaginary part) low-frequency sub-bands and six complex high-frequency sub-bands are generated. The six-complex high-frequency sub-bands are represented in six angles orientations by ±15°, ±45° and ±75°. DTCWT's coefficients represent in the low-frequency most of the visual information of the image, while the high-frequency contains the details and edges of the image only. The imaginary part contains more information compared to the real part which contains less significant data of the host image. [16]. Figure 1 shows the sub-bands of the six complex wavelet coefficients high-frequency and two complex low-frequency coefficients which were obtained from two -level decomposition of the DTCWT transform on the host.

According to Figure 1 which was included as an example, the obtained sub-bands from the two-level decomposition of the DTCWT transform on the host image. The obtained complex coefficients from the decomposed

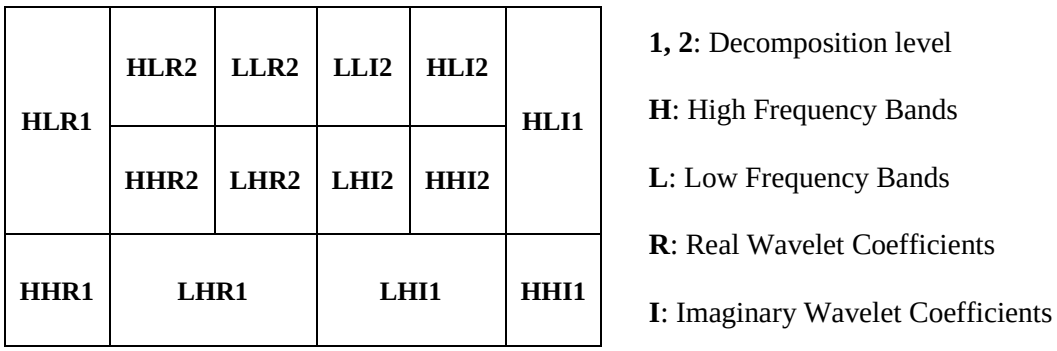

FIGURE 1. - The obtained sub-bands from the two-level decomposition of the DTCWT transform.

image are represented as follows:

$$F_{s,d} = C_{s,d,r} + jC_{s,d,i} \quad (4)$$

Where *s* is the level of decomposition, and *d* denotes directions angles of ±15°, ±45° and ±75° that represent the complex high frequency sub-band whereby $d\epsilon\{1,2,3,4,5,6\}$; *Cs,d,r* and *jCs,d,r* indicates the real (r) and imaginary (i) parts collated when the DTCWT is decomposed using two different trees. Thus, at each level s it produces twelve sub-images that are oriented in ± 75◦, ± 45◦, ± 15◦ and four sub-images at level (s+1) that represent the complex low frequency sub-band that is used for embedding watermark. Therefore, it has been reported to produce good results when used for image watermarking. In addition, its properties are used to preserve ridge angles, and it can strongly deal with geometric attacks.

3.2 DISCRETE COSINE TRANSFORM (DCT)

Discrete Cosine Transform (DCT) is among the most frequent transforms that transform an image to a frequency domain. The most notable DCT description of a 1-Dimension sequence *x* with length *N* is:

$$c(k) = \alpha(k) \sum_{i=0}^{N-1} x(i) \cos\left[\frac{(2i+1)}{2N}\right] \quad (5)$$

Where:

$$\alpha(k) = \begin{cases} \sqrt{2/N} & for \quad k=0 \\ \sqrt{2/N} & for \quad k=1,2..N-1 \end{cases}$$

The corresponding inverse transformation (IDCT) for 1- Dimension sequence *x* with length *N* is:

$$x(i) = \sum_{k=0}^{N-1} \alpha(k) c(k) \cos\left[\frac{(2i+1)k\pi}{2N}\right] \tag{6}$$

Most DCT-based watermarking systems are decomposed into three levels. The level of middle frequency sub-bands contains less information about the host image. Thus, embedding the watermark will be performed by modifying their coefficients without affecting the visual quality of the watermarked image, and the watermark is not removed by compression, unlike the two other levels (lower and higher) of sub-band frequencies which contain the most important visual parts of the image. As a result, components of the image will be removed under the attacks of compression and noise addition [36].

In the proposed method, the image watermarking scheme DTCWT-DCT uses two correlated sub-vectors from DCT-transformed that were generated from DTCWT's coefficients of the whole host image. Then, by using the embedding/extracting differential manner, an optimized embedding is performed with high energy bands of the two generated sub-vectors based on Secant method.

3.3 SECANT METHOD FOR OPTIMIZATION

Numerous researchers have extensively explored and enhanced a Newton's method known as Secant method to accelerate the convergence rate and increase the precision of approximations. Newton's method is an iterative numerical approach that converges quadratically to the solution with each iteration drawing us closer to a solution [11], [13]–[15].

The Secant method's advantages make it demonstrate better overall performance than Newton's method. We can estimate that the secant method uses a finite-difference approximation of Newton's method. So, the Secant method, unlike using an initial guess, begins with two estimates of the root. This method is more stable and less susceptible to variations, and it does not require the calculation of the derivative which could be costly. Typically, the number of iterations needed to achieve the same accuracy is higher compared to the Newton method. However, each iteration is computationally simpler in the secant method [35], [37], [38]. Thus, it can make it suitable for robust watermarking applications that require optimal scaling factors.

The proposed cost function is a combination of PSNR and NC, both of which must be increased in order to achieve robustness and imperceptibility. The parameter is optimized using a variant of Newton's method known as secant method considering an objective function comprising of NC and PSNR; this parameter can be used for watermark implementation by balancing robustness and imperceptibility, and the higher the PNSR is the higher the imperceptibility, the higher the NC is the higher robustness. It implies that we must find a suitable (α) that optimizes (maximizes) both NC and PSNR at the same time. Therefore, NC and PSNR are combined using a suitable scaling factor S, and the cost function is given as (S*NC+PSNR).

In fact, we have maximized (PSNR+S*NC), but for the optimization based on Newton's method, it is required to minimize the cost function. Eventually, we must convert the maximization problem into a minimization function by simply adding a negative sign. Thus, the cost function is given as follows:

$$F(\alpha) = -(S*NC+PSNR) \tag{7}$$

Where: $\alpha \in \mathbb{R}$, and S =scaling factor: e. g S =100. α can be updated using Newton's method by the following formulas:

$$\alpha_{k+1} = \alpha_k - \frac{F'(\alpha_k)}{F''(\alpha_k)} \tag{8}$$

Where: *F'* and *F''* are the first and second derivatives with respect to α, *F'* and *F''* can be given by finite difference method as follows:

$$F'(\alpha) = \frac{F(h+\alpha) - F(\alpha)}{h} \tag{9}$$

$$F''(\alpha) = \frac{F(h+\alpha) + F(h-\alpha) - 2F(\alpha)}{h^2} \tag{10}$$

Where: h is very small (e.g. h=10^{-6}). using equation (9) and equation (10), equation (8) can be rewritten as:

$$\alpha_{k+1} = \alpha_k - \frac{h\left[F\left(h+\alpha_k\right)-F\left(\alpha_k\right)\right]}{F\left(\alpha_k+h\right)+F\left(\alpha_k-h\right)-2F\left(\alpha_k\right)} \tag{11}$$

The obtained optimal scaling factor can be used for watermark embedding to achieve the trade-off between imperceptibility and robustness. Thus, the proposed optimization scheme is used also to identify the best location for embedding watermark in the host image which will be explained in detail in the steps of the proposed optimization scheme in the next part.

4. THE PROPOSED OPTIMIZATION SCHEME DTCWT-DCT

There are three major processes in this proposed watermarking scheme namely the watermark embedding process, the watermark extracting process and the obtaining of optimal scaling factors using Newton's method. The watermarking scheme is started by initializing an optimized value to use during the embedding watermark based on a differential method followed by the watermark embedding process, then the watermark extracting process. Later, Newton's method will find the optimal scaling factor repetitively until the optimal value is reached to achieve the best balance between robustness and imperceptibility through the best of both NC and PSNR obtained values respectively. Each of the major processes is explained in the related subsections below.

4.1 WATERMARK EMBEDDING PROCESS

The proposed embedding process is shown in Figure.2, their proposed algorithm steps can be presented as follows:

Step 1. The input host image (NxN) is subjected to DTCWT decomposition in order to generate the DTCWT coefficients of the host image using the following expression:

$$Z_{m.n} = X_{m.n} + jY_{m.n} \tag{12}$$

Where: X represents the real decomposition coefficients, Y represents the imaginary decomposition coefficients, Z represents the complex decomposition coefficients, and $n=1..N^2/4$ is the total number of coefficients m of decomposition.

Step 2. To keep the adjoining of pixels in one vector as in real images, a zigzag scanning is performed as demonstrated in Figure.3 on the complex coefficients matrix which was obtained from the DTCWT decomposition. The objective is to translate it into a vector of complex coefficients $Z(n)$ to simplify the procedure of embedding watermark into two (correlated) sub-vectors using the differential method, whereby $n=1..N^2/4$, while $N^2/4$ is the magnitude of complex coefficients matrix. The output of the zigzag scanning as shown in Figure.3 is as in Z: Z= {1, 2, 3, …$N^2/4$}

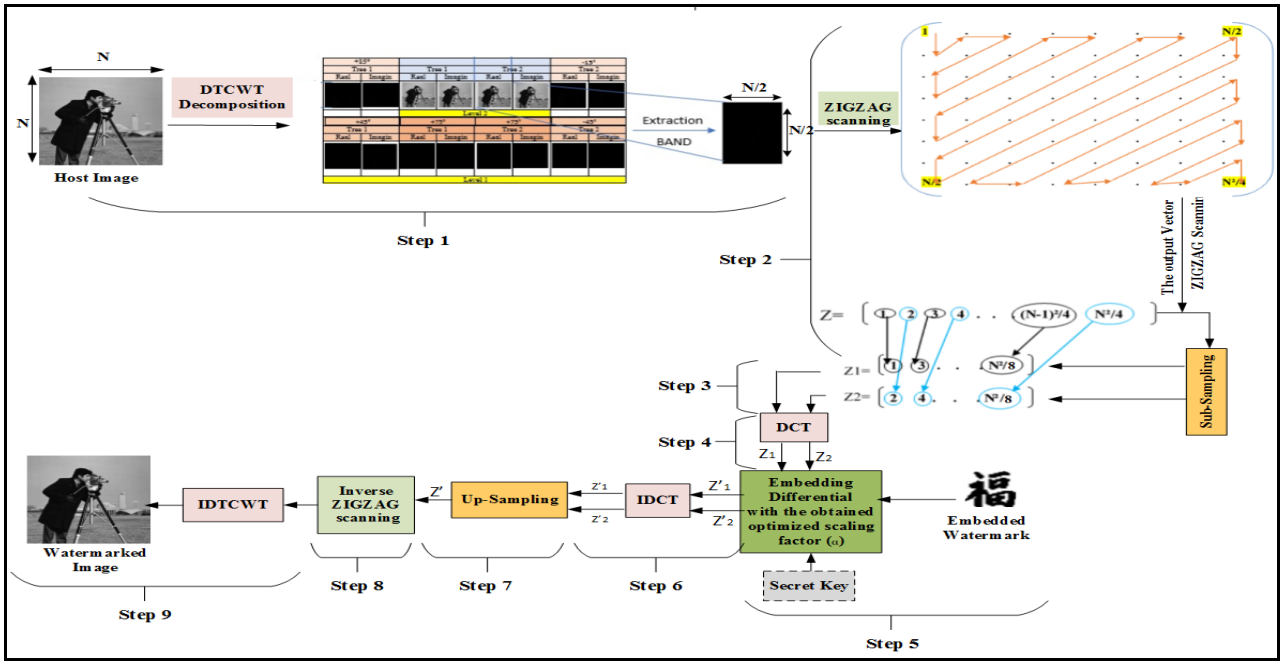

FIGURE 2. - The embedding watermark process

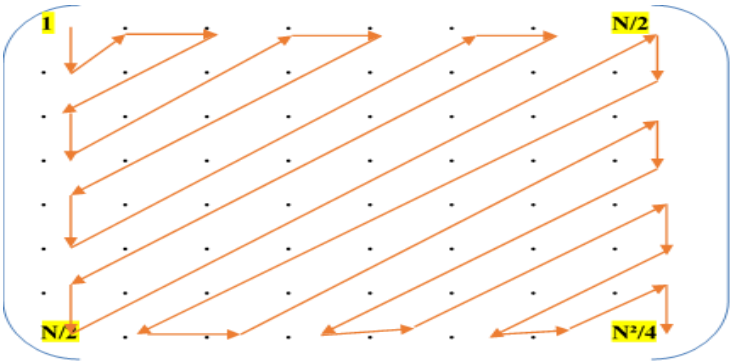

FIGURE 3. - Reading method of the complex coefficient's matrix in a zigzag manner.

Step 3. The coefficients' *Z* vector decomposed into two (correlated) sub-vectors z_1 and z_2 on even and odd index order to use them for differential embedding/extracting method of watermark. This will be explained further in the subsequent section. The decomposition is as follows:

$$z_1(k) = Z(2k) \tag{13}$$

$$z_2(k) = Z(2k-1) \tag{14}$$

Where: $k = 1 \ldots N^2/4$

Step 4. *DCT* is achieved on z_1 and z_2 to produce their altered DCT-transformed z_1 and z_2 that helps to choose the

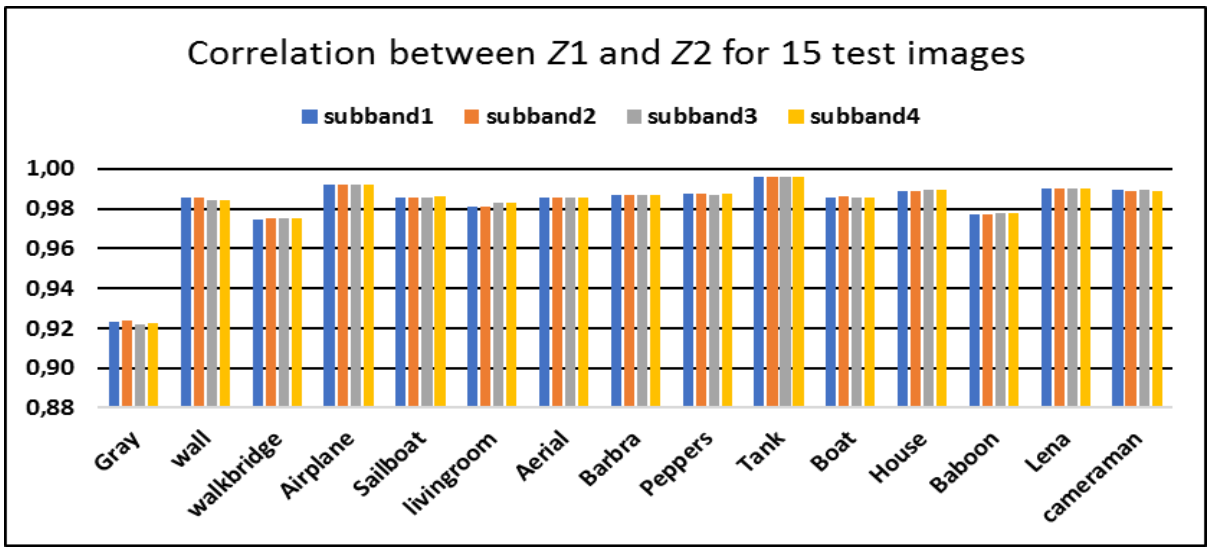

FIGURE 4. - The correlation between DCT- transformed sub-vectors Z1 and Z2 for 15 test images

high energy band of the transformed sub-vectors for differential embedding watermark as shown in Figure.5. The output of two DCT-transformed sub-vectors z_1 and z_2 is described as follows in Equation (15) and Equation (16) respectively:

$$Z_1 = DCT(z_1) \tag{15}$$

$$Z_2 = DCT(z_2) \tag{16}$$

Step 5. A differential embedding approach is used to insert the watermark sequence bits *W(i)* for i= *0,2…L-1*, into vectors Z_1 and Z_2 which have been transformed. This is described by the mathematical Equation (17) and Equation (18) respectively. This allows the incorporation of the watermark indiscriminately into the changed vectors Z_1 and Z_2 acquired from the *DCT* conversion. It is then utilized at the level of mining with no requirement for the original data (blind). Hence, an output of two is created (watermarked) sub-vectors Z'_1 and Z'_2 as follows:

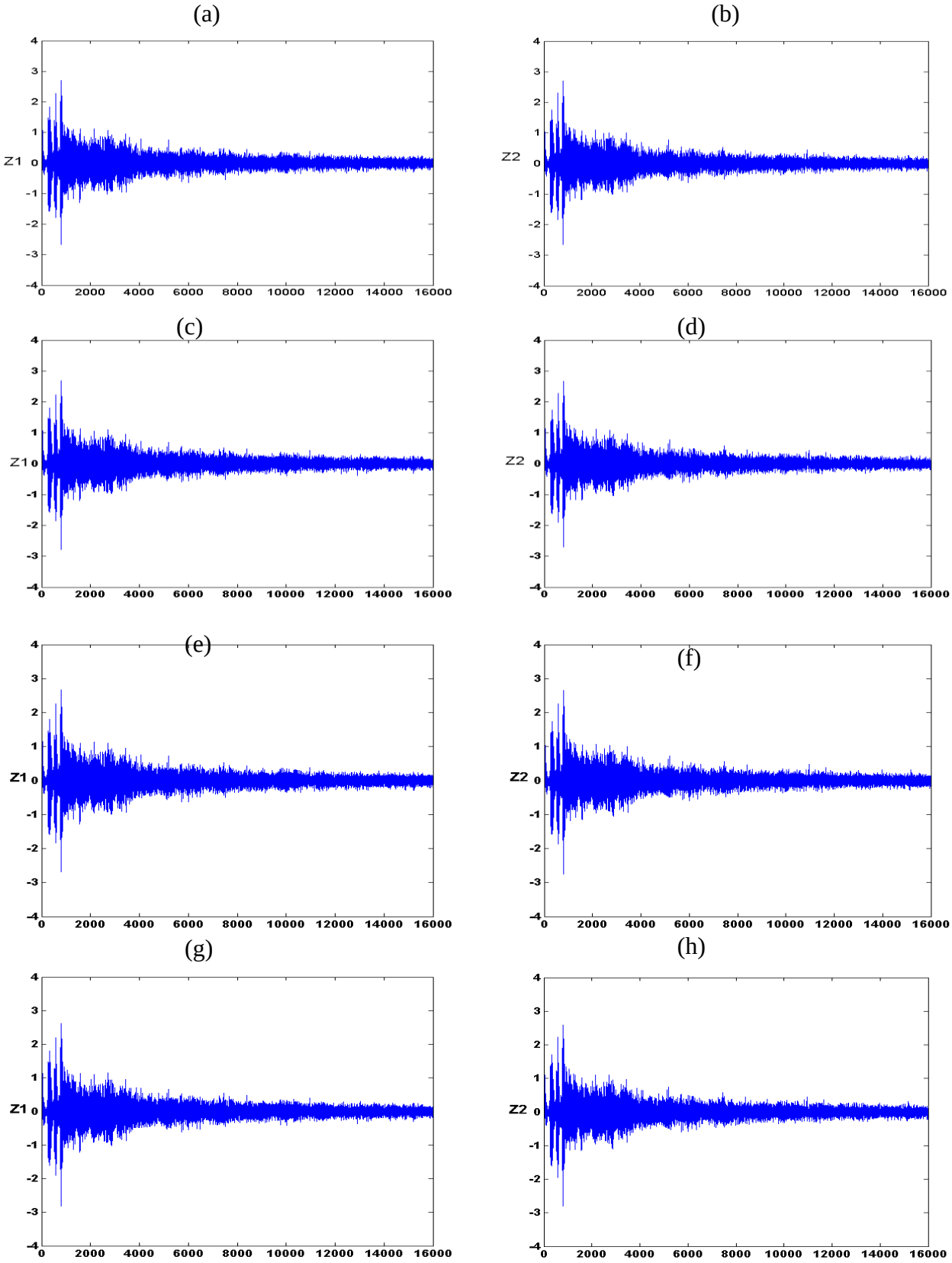

FIGURE 5. - The first half of DCT-transformed sub-vectors Z1 and Z2 (without the DC component) for the image of Lena in four sub-bands of DTCWT decomposition. Sub-band1(a),(b), Sub-band2(c),(d), Sub-band3(e),(f), Sub-band4(g),(h),

$$Z'_1\left(i'\right) = \frac{1}{2}\left[Z_1\left(i'\right) + Z_2\left(i'\right)\right] + \alpha W\left(i\right) \tag{17}$$

$$Z'_2(i') = \frac{1}{2}\left[Z_1(i') + Z_2(i')\right] - \alpha W(i) \tag{18}$$

Where α represents the scaling factor that is used adaptively which enhances the robustness and imperceptibility performance. Finding the optimal scaling factor is through the proposed optimization watermarking steps which will be explained in detail in the next subsection. *i'* represents the random places into the highly strength band of Z_1 and Z_2 which contains the watermark bits. Those represent the components of a vector *r* which can be derived through a random permutation expression as follows:

$$i' = r(i) \tag{19}$$

$$r = RandPerm(S, a, b) \tag{20}$$

Where: *s* represents the seed of the corresponding Pseudo Random Number Generator (PNRG), and *a* and *b* represents the Initial and final points of the applied high strength band are used to incorporate the watermark. Hence, *K= (s, a, b)* is the secret key of the user which would help prevent the watermark from undesirable alterations as well as preventing possible attacks from unauthorized sources.

Step 6. An inverse *DCT* depicted as *IDCT* is performed on Z'_1 and Z'_2 using the following Equation (21) and Equation (22). The purpose of performing the *IDCT* is to reconstruct the vector of complex coefficients *Z'* embedded by watermark.

$$z'_1 = IDCT\left(Z'_1\right) \tag{21}$$

$$z'_2 = IDCT\left(Z'_2\right) \tag{22}$$

Step 7. The two sub-vectors z'_1 and z'_2 are integrated using Equation (23) and Equation (24) so as to create the adjusted vector *Z'* in order to renovate the complex coefficients vector inserted by the watermark.

$$Z'(2k) = z'_1(k) \tag{23}$$

$$Z'(2k-1) = z'_2(k) \tag{24}$$

Where: $k = 1 \ldots N^2/4$.

Step 8. The vector, which has been adjusted vector, is transformed into the matrix with the use of the inverse zigzag scanning which is the inverse process of the method shown in Figure 3 in order to recreate complex a coefficients matrix containing the watermark data.

Step 9. The inverse wavelet transform *IDTCWT* is executed to attain the watermarked image.

4.2 WATERMARK EXTRACTING PROCESS

The proposed extracting process is shown in Figure 6; their proposed algorithm steps can be presented as follows:

Step 1. The implementation of DTCWT on the input watermarked image.

Step 2. The zigzag scanning is performed in order to transform the matrix to a vector of coefficients *Z'*.

Step 3. The vector of coefficients *Z'* is divided into two related sub-vectors z'_1 and z'_2 where the decomposition of sub-vectors is based on Equation (25) and Equation (26).

$$z'_1(k) = Z'(2k) \tag{25}$$

$$z'_2(k) = Z'(2k-1) \tag{26}$$

For: $k = 1 \ldots N^2/4$

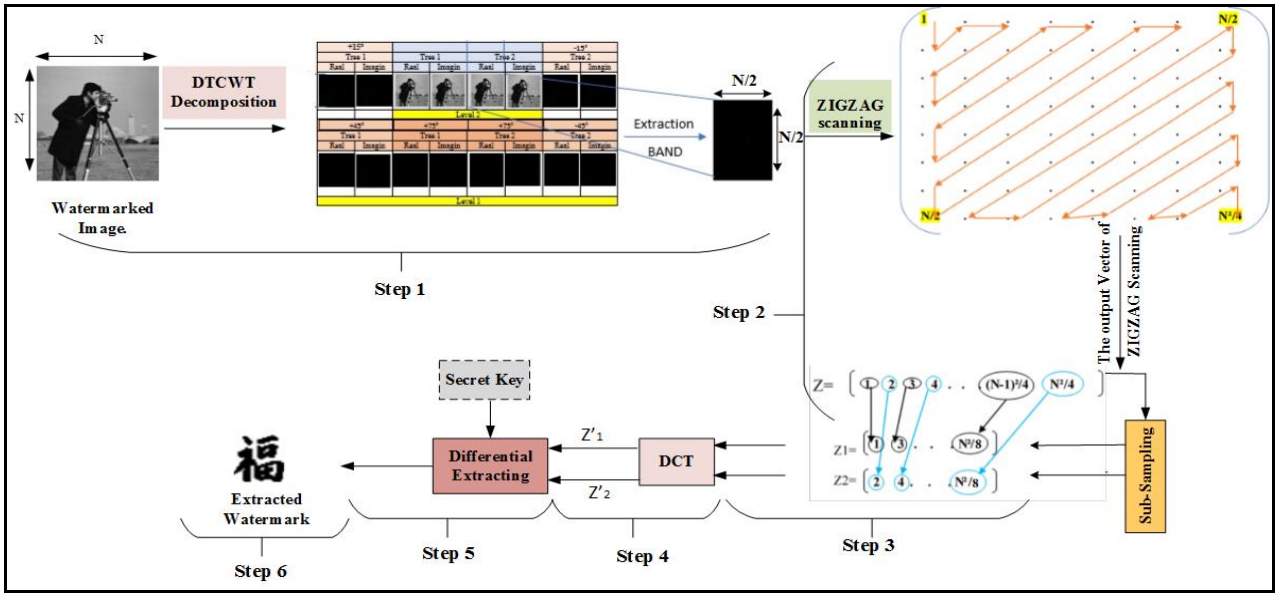

FIGURE 6. - The extracting process.

Step 4. Performing DCT on z'_1 and z'_2 to produce their DCT-transformed forms Z'_1 and Z'_2

$$Z'_1 = DCT\left(z'_1\right) \tag{27}$$

$$Z'_2 = DCT\left(z'_2\right) \tag{28}$$

Step 5. If the watermarked image is entered, then an analogy of the embedding operations will generate two sub-vector Z'_1 and Z'_2 from the extraction operations as proven in Equation (27) and Equation (28) respectively. As such, a proportional difference with the watermark sequence W will be between them as follows:

$$\Delta Z(i) = Z'_1\left(i'\right) - Z'_2\left(i'\right) = 2\alpha W(i) \tag{29}$$

With: $i=1..L$; and i' are the random embedding locations of the watermark bits. These locations are determined through the recreation of vector r, the incorporation of the secret key selected by the selected, and by random permutation as shown in Equation ($Z'_1\left(i'\right) = \frac{1}{2}\left[Z_1\left(i'\right) + Z_2\left(i'\right)\right] + \alpha W(i)$ 17) and Equation (18).

Step 6. Because the difference Δ(i) may vary from (+1/-1) values, a hard limitation function is implemented on it to be able to recover the embedded watermark W' as shown in the following Equation $Z'_1\left(i'\right) = \frac{1}{2}\left[Z_1\left(i'\right) + Z_2\left(i'\right)\right] + \alpha W(i)$ (30):

$$W'(i) = \begin{cases} 1 & if \quad \Delta Z(i) \geq 0 \\ -1 & otherwise \end{cases} \tag{30}$$

4.3 PROCESS TO OBTAIN THE OPTIMAL SCALING FACTOR

The watermarking optimization process is needed in the beginning to assume the initial value of scaling factor α for watermark embedding/extracting process. Then, based on Secant method considering an objective function comprising of *NC* and *PSNR*, the optimal scaling factor *(α)* is found. This obtained optimal scaling factor *(α)* can be used for watermark implementation by balancing robustness and imperceptibility. The steps of the watermarking optimization process are described as shown in Figure .7 as follows:

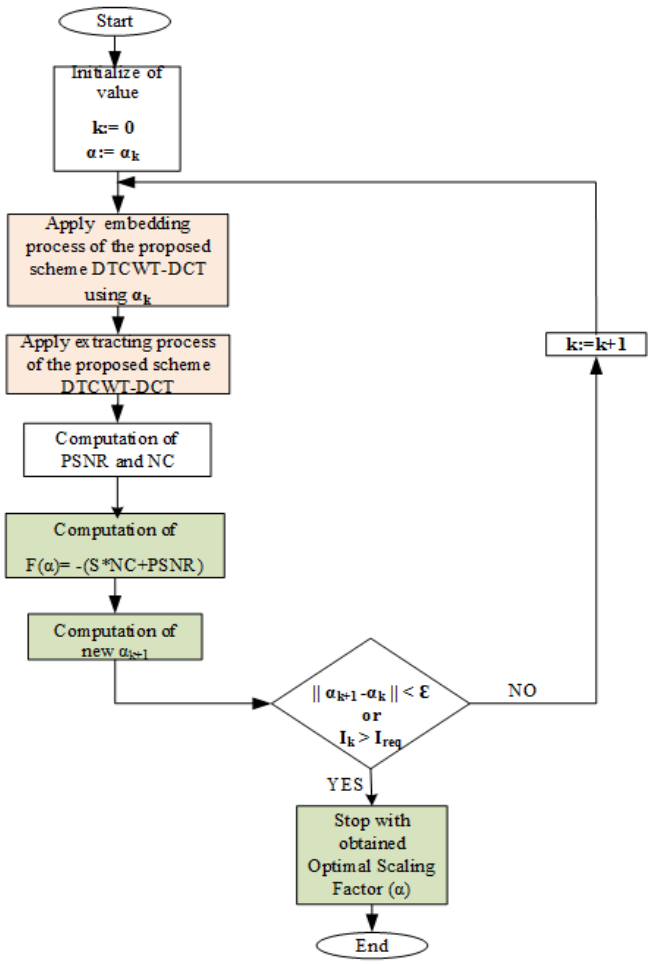

FIGURE 7. - The obtaining of optimal scaling factors(α) using secant method.

Step 1. Initialize the values of the optimized α and the number of iteration *k* by α_0, 0 respectively.

Step 2. Perform the watermark embedding/extracting process using the initial value as shown in Equation (17) and Equation (18). The steps of watermark extracting process will be explained in detail in the next subsection as shown in Figure.6.

Step 3. Compute the values of *NC* and *PSNR* to find the objective function $F(\alpha_k)$ that is shown in Equation (7).

Step 4. Calculate new (α_{k+1}) using Newton's method given by Equation (11).

Step 5. Calculate the absolute value of the difference between the previous value and the new values of the optimized (α), then compare them with epsilon that can be taken as $\epsilon=0.001$.

Step 6. At the end of this step, if the obtained difference from the previous step is less than the imposed epsilon value, the last two obtained values of the optimized scaling factors are deemed equal; this means that convergence has been achieved between the obtained imposed values of optimized (α); the required number of iterations *(Ireq)* for an optimization test is reached; it is determined by running an objective function comprised of *NC* and *PSNR* for a large number of iterations where it will eventually reach a point where any additional iterations will not result in a significant change in the obtained *NC* and *PSNR* values. Hence, no more iterations are required, and it stops the algorithm with an obtained optimized (α). Otherwise, other iterations are required to find optimized (α) through Secant method given by Equation (11).

The obtained optimal scaling factor (α) is used adaptively during the watermark embedding process in order to enhance the trade-off between high imperceptibility and good robustness at the same time.

5. THE EXPERIMENTAL RESULTS

5.1 THE OBTAINED OPTIMAL SCALING FACTOR (A)

To find the optimal scaling factor to use in the proposed image watermarking scheme, an optimization algorithm based on Secant method is proposed. In this experiment that performed implementation through the optimization algorithm, fifteen images of size 512x512 were tested as a host image and a watermark logo of size 32x 32 as an embedded sequence binary watermark. For each host image, it tested the embedding of the watermark in sixteen sub-bands, then it calculated the average of all obtained scaling factor values that will be used as a final optimal scaling factor *(α)* in the embedding watermark process. Table 1 summarises the obtained results of an optimal scaling factor *(α)* in the high/low frequency embedding sub-bands.

Table .1- The optimized scaling factor (α) values in the 16 sub-bands of embedding watermark

Host image	High Frequency sub-band								Low Frequency sub-band							
	1	2	3	4	5	6	7	8	9	10	11	12	13	14	15	16
Cameraman	0,055	0,044	0,003	0,036	0,031	0,005	0,190	0,140	0,005	0,073	0,052	0,013	0,1683	0,1994	0,2103	0,1921
Lena	0,070	0,045	0,017	0,044	0,027	0,028	0,205	0,112	0,026	0,076	0,046	0,052	0,2316	0,2099	0,1827	0,1662
Baboon	0,151	0,152	0,007	0,099	0,030	0,009	0,196	0,301	0,011	0,030	0,146	0,017	0,4144	0,3954	0,3314	0,4310
House	0,114	0,098	0,030	0,074	0,026	0,040	0,249	0,195	0,042	0,108	0,116	0,066	0,2194	0,2199	0,1737	0,1719
Boat	0,162	0,063	0,034	0,124	0,027	0,049	0,386	0,293	0,046	0,183	0,071	0,083	0,2742	0,2444	0,2548	0,2333
Tank	0,066	0,090	0,028	0,061	0,029	0,039	0,157	0,307	0,042	0,074	0,086	0,338	0,1402	0,1513	0,1418	0,1273
Peppers	0,070	0,075	0,026	0,051	0,030	0,041	0,121	0,167	0,036	0,075	0,077	0,080	0,2681	0,2538	0,2383	0,2078
Barbra	0,337	0,062	0,040	0,263	0,028	0,072	0,482	0,146	0,080	0,396	0,058	0,303	0,2567	0,2923	0,2883	0,2990
Aerial	0,140	0,150	0,039	0,069	0,029	0,045	0,289	0,265	0,052	0,136	0,176	0,125	0,4144	0,3516	0,3837	0,4170
Livingroom	0,123	0,142	0,052	0,084	0,029	0,062	0,302	0,289	0,066	0,147	0,138	0,147	0,2411	0,2760	0,2286	0,2393
Sailboat	0,108	0,079	0,032	0,089	0,029	0,045	0,266	0,195	0,045	0,124	0,083	0,093	0,2441	0,2706	0,2370	0,2467
Airplane	0,088	0,083	0,013	0,050	0,036	0,021	0,202	0,247	0,018	0,103	0,075	0,039	0,2436	0,2438	0,2661	0,2145
Walkbridge	0,153	0,192	0,060	0,099	0,121	0,080	0,386	0,286	0,073	0,161	0,175	0,159	0,3413	0,3161	0,3474	0,3516
Wall	0,166	0,125	0,050	0,111	0,027	0,071	0,995	0,279	0,079	0,176	0,108	0,147	0,2186	0,2438	0,2171	0,2561
Gray	0,389	0,292	0,063	0,237	0,025	0,078	1,016	0,544	0,094	0,354	0,261	0,378	0,5974	0,8102	0,6582	0,4291
Average	0,146	0,113	0,033	0,099	0,035	0,046	0,363	0,251	0,048	0,148	0,111	0,136	0,2849	0,2986	0,2773	0,2655

5.2 IMPERCEPTIBILITY PERFORMANCE FOR THE WATERMARKED IMAGES.

In this section, the performance of the optimization proposed DTCWT-DCT scheme for watermark embedding process was tested through measuring the imperceptibility value of the watermarked image (PSNR and SSIM values) on the fifteen different images. Table.2 shows the obtained results of average PSNR and SSIM values into sixteen sub-bands of embedding for each tested image.

Referring to Table.2, a high imperceptibility in most of the sixteen sub-bands of embedding watermark was achieved, especially in the high frequency sub-bands that achieved PSNR value greater than 45dB for all the tested images. This introduces an additional advantage for improving the security of watermark embedding.

Table 2. - PSNR and SSIM values of the optimization proposed DTCWT-DCT scheme.

Host Image	High Frequency sub-band		Low Frequency sub-band	
	PSNR	SSIM	PSNR	SSIM
Camera	45,238	0,978	38,054	0,910
Lena	45,216	0,982	38,069	0,926
Baboon	45,178	0,993	38,023	0,969
Goldhill	45,206	0,989	38,081	0,950
Boat	45,173	0,988	38,022	0,948
Tank	45,218	0,987	38,086	0,945
Peppers	45,236	0,984	38,040	0,932
Barbara	45,042	0,988	38,047	0,951
Aerial	45,159	0,992	37,949	0,963
Couple	45,175	0,987	38,051	0,945
Pirate	45,205	0,988	38,030	0,945
Jet plane	45,201	0,982	38,037	0,923
Bridge	45,150	0,994	38,036	0,975
wall	45,163	0,994	38,036	0,974
Gray	44,910	0,999	37,690	0,996
Average	45,165	0,988	38,017	0,950

COMPARISON OF IMPERCEPTIBILITY PERFORMANCE WITH OTHER SCHEMES

This section provides a comparison of the performance of imperceptibility between the optimization proposed DTCWT-DCT scheme and the existing work. Table .3 summarizes the comparison of schemes proposed by Makbol et al., (2016), Ernawan et al., (2018) and Ariatmanto et al., (2020) and the optimization proposed DTCWT-DCT scheme.

Table 3. - Comparisons with schemes proposed by Makbol et al., (2016), Ernawan et al., (2018) and Ariatmanto et al., (2020) in terms of PSNR and SSIM values.

Host image	[6]		[5]		[39]		Proposed scheme	
	PSNR	SSIM	PSNR	SSIM	PSNR	SSIM	PSNR	SSIM
Lena	44.824	0.980	45.689	0.993	**45.731**	**0.994**	45,216	0,982
Airplane	42.046	0.954	45.533	**0.994**	**43.488**	0.988	45,201	0,982
Baboon	43.301	0.986	45.495	0.995	**45.682**	**0.996**	45,178	0,993
House	41.944	0.957	44.546	**0.995**	43.830	0.989	**45,206**	0,989
Barbara	43.697	0.986	45.689	0.994	**47.818**	**0.997**	45,042	0,988
Boat	44.805	0.975	45.163	0.993	**46.339**	**0.994**	45,173	0,988
Peppers	43.889	0.981	44.858	**0.996**	**45.953**	0.995	45,236	0,984
Sailboat	42.479	0.965	44.498	**0.997**	43.796	**0.990**	**45,205**	0,988
Average	43.373	0.973	45.381	0.995	45.330	0.993	45,182	0,987

As shown in Table.3, The obtained PSNR and SSIM values are the average PSNR and SSIM values from the embedding watermark process of the optimization proposed DTCWT-DCT scheme. The performance of imperceptibility was introduced in terms of PSNR and SSIM values for all eight tested images by 45 dB and 0,98 respectively. It achieved the highest performance of imperceptibility in term of PSNR value for House and Sailboat host images compared to the proposed schemes by Ariatmanto et al.,(2020), Ernawan et al., (2018) and Makbol et al., (2016). Whilst the scheme by (Ariatmanto et al., 2020) outperformed under the other test images. The Figure.8. presents the visual comparison of the average PSNR values for the optimization proposed DTCWT-DCT scheme compared to the proposed schemes by Ariatmanto et al., (2020), Makbol et al., (2016) and Ernawan et al., (2018).

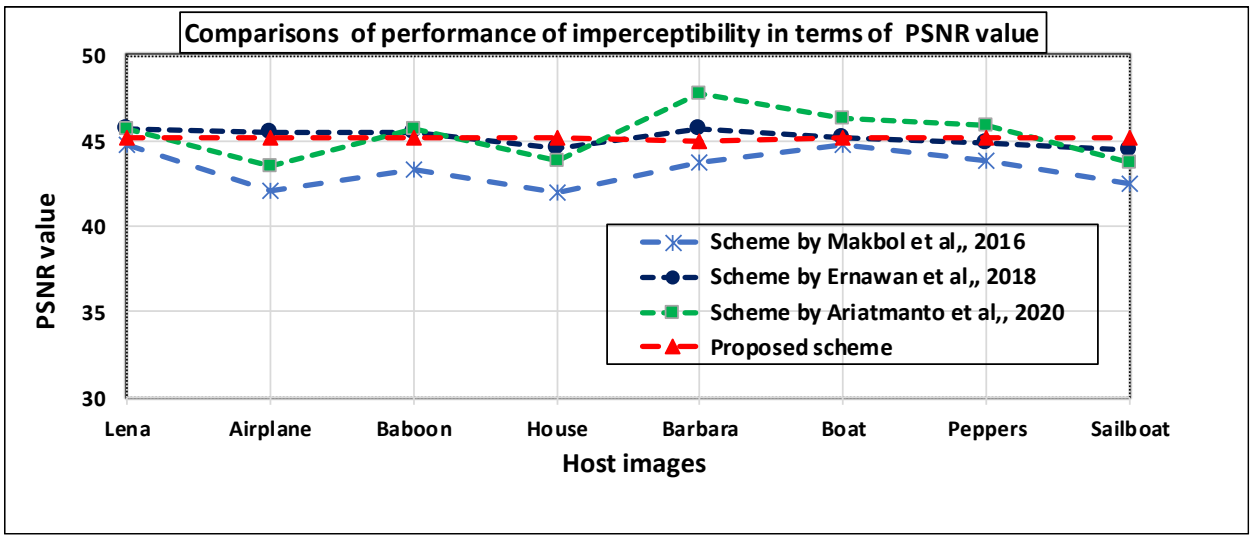

FIGURE 8. - Comparison of performance of imperceptibility in terms of PSNR value of the watermarked images.

Based on Figure.8, the optimization proposed DTCWT-DCT scheme achieves the highest performance of imperceptibility for the House and Sailboat images compared to the proposed schemes by Ariatmanto et al., (2020), Makbol et al., (2016) and Ernawan et al., (2018), except the scheme introduced by Ariatmanto et al., (2020) outperformed under the others tested images.

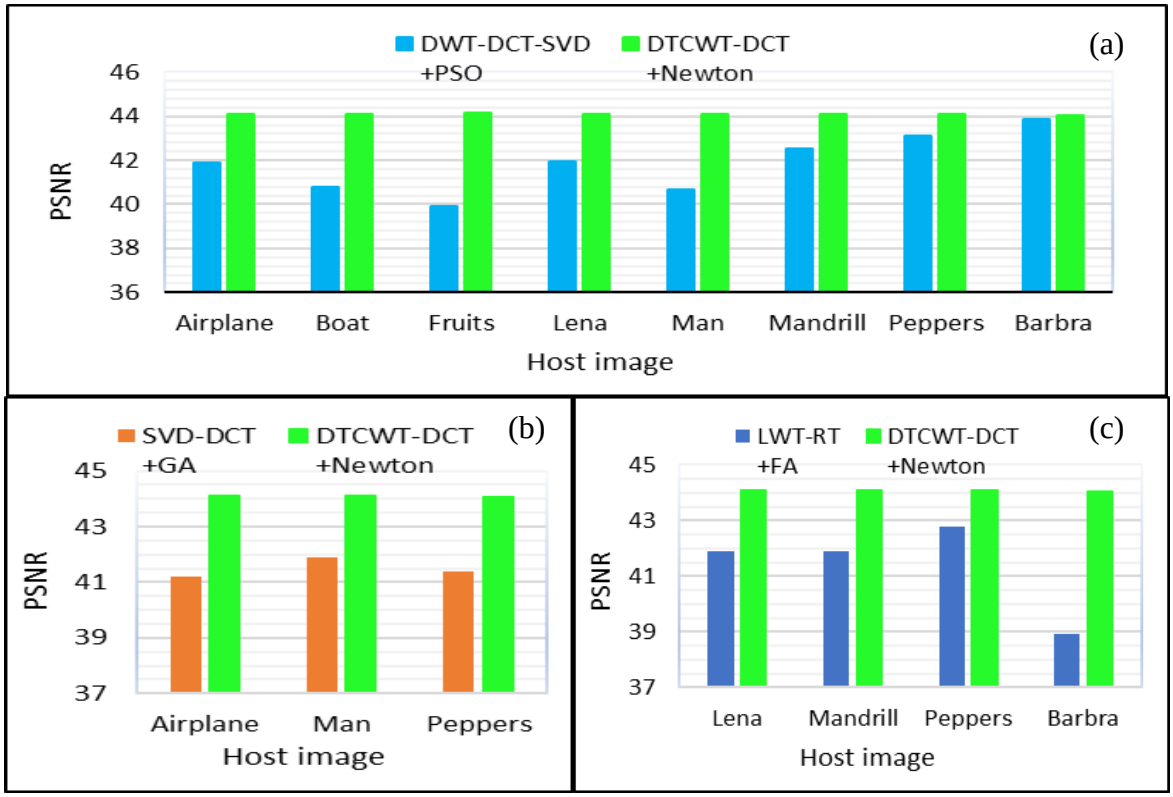

FIGURE 9. - Imperceptibility comparison in terms of PSNR value of the watermarked images between the optimization proposed DTCWT-DCT scheme and existing schemes proposed by (a)Kanget al. (2020)., (b)Kazemivash et al., (2018)., (c)Han et al. (2016).

The performance of imperceptibility for the optimization proposed scheme DTCWT-DCT is compared also with the other existing watermarking schemes that were combined between the hybrid domain and the optimization methods. Figure.9. presents the visual comparison of the average PSNR values for the optimization proposed DTCWT-DCT scheme compared to the proposed schemes by Kazemivash et al., (2018), Han et al. (2016) and Kanget al. (2020).

Referring to Figure.9, the proposed scheme achieved the highest performance of imperceptibility in term PSNR value by an average of 45 dB for all tested images compared to the proposed schemes by Kazemivash et al., (2018), Han et al. (2016) and Kanget al. (2020). It means that the proposed scheme performs better in terms of imperceptibility for the watermarked image.

5.3 ROBUSTNESS PERFORMANCE FOR THE RECOVERED WATERMARK

Measurement of the robustness performance for the recovered watermark of the optimization proposed DTCWT-DCT scheme is presented in this section. The performance of the optimization proposed DTCWT-DCT scheme was measured against common digital image watermarking attacks. Table.4 summarises the abbreviations of the different attacks types with the values of their test used in the proposed scheme.

Table 4. - Abbreviation attacks with the values of their test

Abbreviation	Description of attack With value of its test	Abbreviation	Description of attack With value of its test
GN001	Gaussian Noise, variance = 0.001	JPEG2000 CR=10	JPEG 2000 with Compression Ratio = 10
GN005	Gaussian Noise, variance = 0.005	CO25	Cropping Off 25%
SP001	Salt and Pepper Noise density = 0.001	CO50	Cropping Off 50%
SP005	Salt and Pepper Noise density = 0.005	CC25	Centered Cropping 25%
SP03	Salt and Pepper Noise density = 0.03	CC50	Centered Cropping 50%
SP01	Salt and Pepper Noise density = 0.01	CRO25	Cropping Row Off 25%
SN001	Speckle noise, density =0.001	CRO50	Cropping Row Off 50%
SN005	Speckle noise, density = 0.005	CCO25	Cropping Column Off 25%
SH	Sharpening	CCO50	Cropping Column Off 50%
HE	Histogram Equalization	SC08	Scaling 0.8
JPEGQ50	JPEG with quality factor = 50	AF [3,3]	Average Filter [3 3]
JPEGQ60	JPEG with quality factor = 60	GF [3,3]	Gaussian Filter [3 3]
JPEGQ70	JPEG with quality factor = 70	MF [3,3]	Median Filter[3 3]
JPEGQ75	JPEG with quality factor = 75	WF [3,3]	Wiener Filter [3 3]
JPEGQ80	JPEG with quality factor = 80	GF [3,3]	Gaussian Filter [3 3] (sigma:0,05)
JPEGQ90	JPEG with quality factor = 90	GF [3,3]	Gaussian Filter [3 3] (sigma:0,1)
JPEGQ100	JPEG with quality factor = 100	GF [3,3]	Gaussian Filter [3 3] (sigma:0,2)
JPEG2000 CR=2	JPEG 2000 with Compression Ratio = 2	GF [3,3]	Gaussian Filter [3 3] (sigma:1,0)
JPEG2000 CR=4	JPEG 2000 with Compression Ratio = 4	GB	Gaussian Blur
JPEG2000 CR=6	JPEG 2000 with Compression Ratio = 6	BC	Brightness and Contrast
JPEG2000 CR=8	JPEG 2000 with Compression Ratio = 8	RD	Rotation Degree, Degree=5°

Table 5. - NC values of the optimization proposed DTCWT-DCT scheme against various noise attacks.

Host Image	GN001	GN005	SP001	SP005	SP03	SN001	SN005	SH	HE
Lena	0,9620	0,9587	1,0000	0,9990	0,9624	**1,0000**	0,9971	1,0000	1,0000
Baboon	0,9128	0,9116	0,9657	0,9571	0,9297	0,9638	0,9602	0,9710	0,9410
House	0,9614	0,9494	0,9990	0,9980	0,9656	1,0000	0,9990	1,0000	0,9971
Boat	0,9460	0,9517	0,9980	0,9971	0,9530	0,9971	0,9961	0,9971	1,0000
Peppers	0,9602	0,9473	0,9961	0,9951	0,9500	0,9980	0,9971	0,9990	1,0000
Barbra	0,9407	0,9430	0,9922	0,9813	0,9512	0,9932	0,9922	0,9961	0,9941
Airplane	0,9426	0,9500	0,9980	0,9892	0,9417	1,0000	0,9912	0,9990	1,0000
Sailboat	0,9441	0,9453	0,9971	0,9922	0,9459	0,9951	0,9932	1,0000	0,9980

The results in Table.5 indicate that the optimization proposed DTCWT-DCT scheme is adequately robust against the four groups of noise attacks (salt and pepper, Speckle, sharpening and histogram equalisation) despite the high-density noises. The optimization proposed DTCWT-DCT scheme attained an accepted result of NC values above 0.99 for the most tested images except for Gaussian noise attack which achieved an NC value less than 0.95. Therefore, it can be said that the proposed technique exhibits good robustness against these types of attacks.

The NC values of the extracted watermarks under JPEG and JPEG2000 compression attacks are given in Table.6. JPEG compression was tested on different watermarked images by the various quality factors (Q) which varies from 50 to 90, while JPEG2000 was tested on the compression ratio (CR) that varies from 2 to 10.

Table 6. - NC values of the optimization proposed DTCWT-DCT scheme against compression attacks.

Host Image	JPEG Q 50	JPEG Q 60	JPEG Q 70	JPEG Q 80	JPEG Q 90	JPEG 2000 (CR2)	JPEG 2000 (CR4)	JPEG 2000 (CR6)	JPEG 2000 (CR8)	JPEG 2000 (CR10)
Lena	0,9980	0,9990	0,9990	0,9990	1,0000	1,0000	1,0000	0,9971	0,9941	0,9844
Baboon	0,9497	0,9486	0,9493	0,9512	0,9608	0,9497	0,9476	0,9102	0,9010	0,8734
House	0,9961	0,9971	0,9990	0,9980	1,0000	1,0000	1,0000	0,9941	0,9922	0,9883
Boat	0,9931	0,9941	0,9951	0,9941	0,9990	0,9990	0,9942	0,9793	0,9667	0,9440
Peppers	0,9863	0,9921	0,9941	0,9951	0,9980	0,9961	0,9961	0,9892	0,9784	0,9648
Barbra	0,9795	0,9912	0,9932	0,9941	0,9961	0,9951	0,9922	0,9697	0,9468	0,8696
Airplane	0,9912	0,9912	0,9951	0,9980	0,9980	0,9971	0,9971	0,9951	0,9735	0,9676
Sailboat	0,9854	0,9951	0,9961	0,9961	0,9980	1,0000	0,9961	0,9863	0,9609	0,9454

Referring to Table 6, the NC value for most eight tested images was more than 0.99 under various test quality factors (Q) of JPEG compression except Baboon image which achieved NC values less than 0.96 for all various quality factors of JPEG compression attack. Whereas JPEG2000 under compression ratio (CR) between 2 and 6, most tested images achieved an NC value greater than 0.99 except Baboon image whose NC value was less than 0.95. When applying a value more than 6 for compression ratio (CR), the NC value for most eight tested images nearly falls between 0.94 and 0.98 except for Baboon and Barbra images which attained 0,87 of NC value under value 10 of compression ratio (CR).

The results shown in Table.6 indicate that the extracted watermark is fully recovered in JPEG2000 and JPEG compression when using values less than 6 and more than 50 for the compression ratio (CR) and the quality factor (Q) respectively. Thus, it can be concluded from the acceptable results obtained for JPEG and JPEG2000 compression that the optimization proposed DTCWT-DCT scheme has proven good performances against those types of attacks.

The types of geometric attacks which were tested are resizing with the resizing factor (Q = 0.8) and various types of cropping CO (25% and 50%), CC (25% and 50%), CRO (25% and 50%) and CCO (25% and 50%), and the results are presented in the Table.7.

The data shown in Table .7 reveal that the obtained NC values from the resizing attack with the resizing factor (Q = 0.8) were greater than 0.99 on all tested images except Baboon image which achieved NC values less than 0.95. As for the type of cropping attack (CO25% and CC 25%), the obtained NC values from most tested images were greater than 0.99 apart from Baboon image which attained NC values 0.96 and 0.92 under CO25% and CC 25% respectively while the NC values ranged between 0.92 and 0.98 in most tested images under the type of cropping attack (CO50%, CC50%, CRO25% and CCO25%) aside from Baboon image that achieved for NC values 0,90 and 0,86 under CO50% and CC 50% respectively. As concerns the type of cropping attack (CRO50% and CCO 50%), the obtained NC values from most tested images were less than 0.92.

Table 7. - NC values of the optimization proposed DTCWT-DCT scheme against geometrical attacks.

Host Image	CO 25%	CO 50%	CC 25%	CC 50%	CRO 25%	CRO 50%	CCO 25%	CCO 50%	SC 0.8
Lena	0,9990	0,9804	0,9941	0,9706	0,9754	0,9061	0,9814	0,9218	1,0000
Baboon	0,9641	0,9092	0,9264	0,8628	0,9091	0,8536	0,9185	0,8431	0,9498
House	0,9932	0,9794	0,9971	0,9679	0,9707	0,9265	0,9834	0,9389	0,9980
Boat	0,9863	0,9493	0,9912	0,9452	0,9497	0,8830	0,9560	0,8608	0,9951
Peppers	0,9980	0,9708	0,9932	0,9617	0,9715	0,9171	0,9697	0,9103	0,9892
Barbra	0,9824	0,9452	0,9805	0,9365	0,9419	0,8742	0,9541	0,8906	0,9931
Airplane	0,9902	0,9554	0,9833	0,9285	0,9474	0,8789	0,9639	0,8743	0,9932
Sailboat	0,9961	0,9786	0,9922	0,9328	0,9706	0,8944	0,9689	0,9220	0,9921

Based on the results discussed in Table .7, it can be concluded that DTCWT-DCT scheme could almost be able to fully recover the watermark against the shown tested geometrical attacks. While against the cropping attack type (CO50%, CC50%, CRO25% and CCO25%), the technique exhibits less performance than expected because the rate of grand cropping causes severe degradation of the watermarked image and recovered watermark.

5.4 COMPARISON OF ROBUSTNESS PERFORMANCE WITH OTHER SCHEMES IN TERMS OF NC VALUE

In this section, a comparison of the robustness performance of the recovered watermark of the optimization proposed DTCWT-DCT scheme with other schemes was presented. In this experiment, an image Lena of size 512×512 pixels as a host image and a logo watermark of size 32×32 pixels as an embedded watermark were tested.

Based on Table .8, the optimization proposed DTCWT-DCT scheme was able to achieve higher robustness of the recovered watermark than the schemes introduced by (Lyu et al., 2014) and (Ariatmanto et al., 2020) under Salt and Pepper Noise attack with various densities (0.001, 0.005 and 0.1) and cropping attack of the type CO with (25%).

Table 8. - Comparisons with schemes proposed by Lyu et al., (2014) and Ariatmanto et al., (2020) in terms of NC value under various attacks.

Attacks	[40]	[39]	Proposed scheme
SP001	0,9803	0,9883	**1,0000**
SP005	0,9698	0,9581	**0,9990**
SP01	0,9494	0,9242	**0,9756**
JPEGQ 100	0,9818	**1,0000**	**1,0000**
GF 3 × 3 (sigma: 0.05)	0,9818	**1,0000**	**1,0000**
GF 3 × 3 (sigma: 0.1)	0,9818	**1,0000**	**1,0000**
GF 3 × 3 (sigma: 0.2)	0,9818	**1,0000**	**1,0000**
CO 25%	0,9743	0,9730	**0,9990**

Further, the optimization proposed DTCWT-DCT scheme was able to fully recover the watermark under JPEG compression with quality factor (100) and different variance values of Gaussian filter (3×3). Thus, it can be concluded that the proposed DTCWT-DCT watermarking scheme enhanced robustness against this type of attacks as shown in Figure .10.

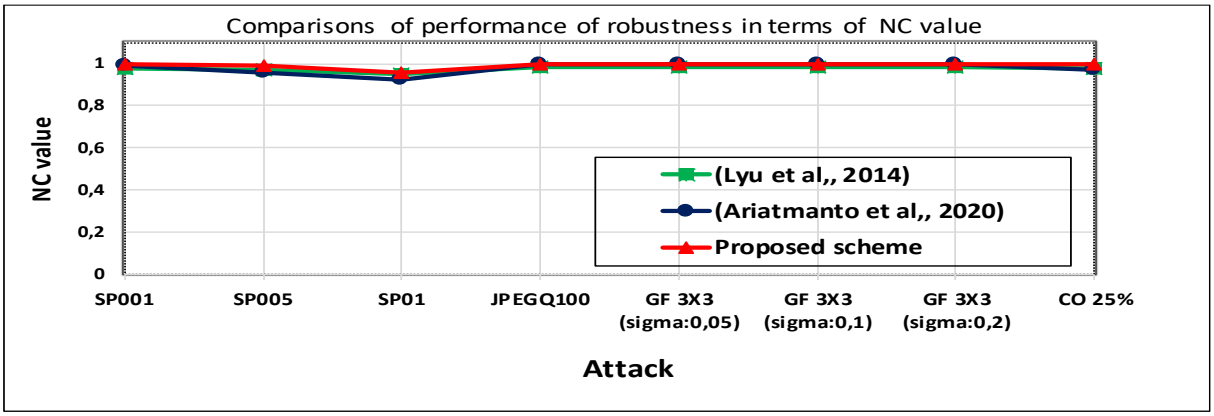

FIGURE 10. - Comparisons with schemes proposed by Lyu et al., (2014) and Ariatmanto et al., (2020) in terms of NC value under various attacks.

The optimization proposed DTCWT-DCT scheme was compared to other schemes under other types of image processing attacks such as low-pass filtering attacks. Table .9 summarises the comparison of the obtained results of NC value between our optimization proposed DTCWT-DCT scheme and the schemes proposed by Makbol et al., (2016), Tagesse Takore et al., (2018), Mehta et al., (2016) and Ariatmanto et al., (2020) as follows:

Table 9. - Comparisons with (Lyu et al., 2014 and Ariatmanto et al., 2020) schemes in terms of NC value under various attacks.

Attacks	[6]	[41]	[42]	[39]	**Proposed scheme**
AF[3,3]	0,7021	0,9268	0,9357	**1,0000**	0,9566
GF[3,3]	0,9971	0,9576	0,9930	**1,0000**	0,9980
MF[3,3]	0,9131	0,9466	0,9984	**0,9971**	0,9747
WF[3,3]	0,7080	0,9451	1,0000	**1,0000**	0,9677
HE	0,9922	0,8449	0,9984	**1,0000**	**1,0000**
JPEG50	0,9688	0,9787	**1,0000**	0,9961	0,9980
SH	0,9971	0,9915	0,9399	**1,0000**	**1,0000**

As shown in Table.9, the optimization proposed DTCWT-DCT scheme achieved higher NC values for all tested types attacks types apart from low-pass filtering attacks, wherever, the superiority in them was through the scheme proposed by (Mehta et al., 2016) under median filter(MF) and compression JPEG with quality factors (Q=50). In addition, the scheme proposed by (Ariatmanto et al., 2020) outperformed under average filter (AF), gaussian filter (GF)and wiener filters (WF). The aforementioned discussed results demonstrate that the optimization proposed DTCWT-DCT scheme fulfilled more robustness for the recovered watermark against histogram equalisation (HE) and sharpening (SH) while it decreased against filtered of the image.

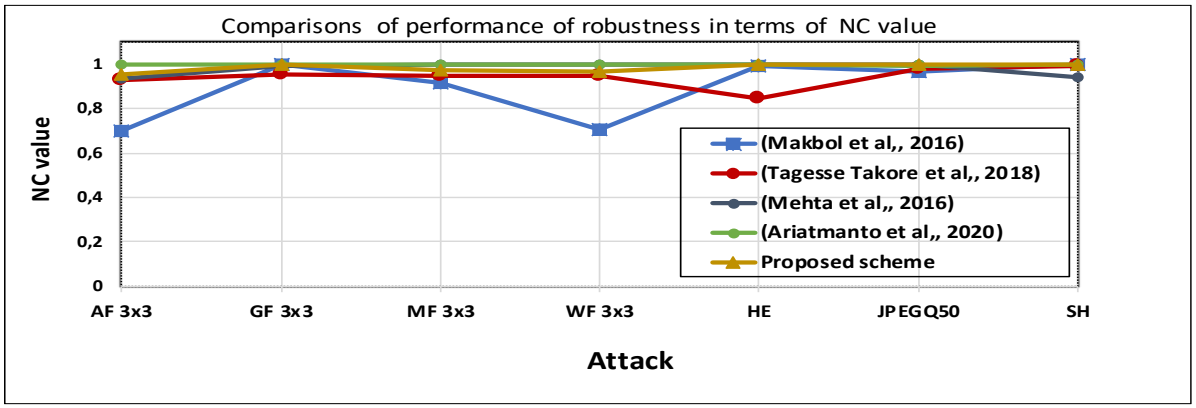

FIGURE 11.- Comparisons with (Makbol et al., 2016, Tagesse Takore et al., 2018, Mehta et al., 2016 and Ariatmanto et al., 2020) schemes in terms of NC value under various attacks.

Figure.11 illustrates a comparison between the optimization proposed DTCWT-DCT scheme and the proposed schemes by Makbol et al., (2016), Mehta et al., (2016), Tagesse Takore et al., (2018) and Ariatmanto et al., (2020) in terms of NC value under various attacks.

The evaluation of robustness performance for the optimization proposed DTCWT-DCT scheme was also tested under other different types of attacks and then compared with other recent image watermarking schemes. The proposed schemes were introduced by Agarwal et al., (2013), Mehta et al., (2016) and Ariatmanto et al., (2020) to be compared with the optimization proposed DTCWT-DCT scheme. The obtained results of NC values were summarized in Table .10 as follows.

Table 10.- Comparisons with (Agarwal et al., 2013, Mehta et al., 2016 and Ariatmanto et al., 2020) schemes in terms of NC value under various attacks.

Attacks	Lena				Baboon			
	[43]	[42]	[39]	**Proposed scheme**	[43]	[42]	[39]	**Proposed scheme**
PSNR	37.6345	45.7241	**45.7313**	38,0668	37.5532	43.1230	**45.682**	38,0050
GB	0.9442	0.9903	**1,0000**	0,9980	0.9323	0.9618	**0.9971**	0,9451
MF (3 × 3)	0.9013	**0.9984**	0.9971	0,9747	0.9006	0.9428	**0.9747**	0,9243
WF (3 × 3)	0.934	**1,0000**	**1,0000**	0,9677	0.9189	0.9356	**0.9844**	0,8929
BC	**1,0000**	0.9984	**1,0000**	0,9980	**1,0000**	0.9752	0.9990	0,9716
SC	**1,0000**	0.9905	**1,0000**	**1,0000**	**1,0000**	0.9419	0.9980	0,9498
JPEGQ 90	**1,0000**	**1,0000**	**1,0000**	**1,0000**	**1,0000**	0.9729	1,0000	0,9608
JPEGQ 75	**1,0000**	**1,0000**	**1,0000**	0,9990	**1,0000**	0.9729	0.9980	0,9618
JPEGQ 50	**1,0000**	1,0000	0.9961	**0,9980**	**1,0000**	0.9729	0.9204	0,9497

Based on Table.10, Although, the optimization proposed DTCWT-DCT scheme reveals a lower PSNR value compared to the schemes proposed by Mehta et al., (2016) and Ariatmanto et al., (2020). However, it attained higher NC values greater than 0.99 under BC, SC, JPEGQ 90, JPEGQ 75 and JPEGQ 50 attacks with Lena image. Those results exclude Baboon image where the obtained NC values under these types of attacks were less than 0.97, while the schemes proposed by Ariatmanto et al., 2020 and Agarwal et al., 2013 outperformed under GB, MF (3 × 3) and WF (3 × 3) attacks, and BC, SC, JPEGQ 90 and JPEGQ 75 attacks for both Lena and Baboon images respectively. Those results lead us to conclude that the optimization proposed DTCWT-DCT scheme demonstrates robustness for the recovered watermark against BC, SC, JPEGQ 90, JPEGQ 75 and JPEGQ 50 aside from filtered of the image which reveals less robustness.

The proposed optimization scheme DTCWT-DCT was compared as well to the related watermarking schemes which used a combination of hybrid domain and optimization methods. It was tested under Gaussian noise attack in the density of 0.001, median filter (MF) (3×3), and JPEG compression with the quality factor (QF=60). Table .11 summarizes the obtained results of the comparison of NC value between the proposed scheme and the schemes proposed by Han et al. (2016) and Kang et al. (2020) as follows:

Table 11.- Comparisons with schemes proposed by Han et al. (2016) and Kang et al. (2020) schemes in terms of NC value under various attacks.

Attacks	GN001			MF (3 × 3)			JPEGQ60		
	[44]	[21]	**Proposed scheme**	[44]	[21]	**Proposed scheme**	[44]	[21]	**Proposed scheme**
Lena	0,9275	0,8757	0,9738	0,8798	0,9893	1	0,8788	0,9666	1
Mandrill	0,9167	0,9505	0,9696	0,8299	0,999	1	0,8374	0,9932	1
Barbara	0,8987	0,9961	0,9546	0,8423	0,9961	0,9669	0,8473	1	0,9727
Peppers	0,9253	0,9693	0,9676	0,8343	0,9971	0,9990	0,8776	1	1
Airplane	0,9135	0,8958	0,9696	0,8294	0,999	1	0,8976	0,9582	0,9990

Based on Table .11, the proposed optimization scheme DTCWT-DCT was able to attain robustness of the recovered watermark higher than schemes introduced by Han et al. (2016) and Kang et al. (2020) with the tested images (Lena, Mandrill and Airplane) under Gaussian noise attack in the density of 0.001, median filter (MF) (3×3), and JPEG compression by the quality factor (QF=60). As for the image Barbara, the scheme presented by Kang et al. (2020) outperformed the other schemes under all tested attacks. Thus, it can be concluded that the scheme had enhanced robustness against this type of attacks.

In the next section, the proposed DTCWT-DCT scheme was also compared with other schemes under various types of image processing attacks based on the measurement of bit error rate (BER) to evaluate of robustness of the recovered watermark.

5.5 COMPARISON OF ROBUSTNESS PERFORMANCE WITH OTHER SCHEMES IN TERMS OF BER VALUE

The bit error ratio (BER) is another parameter to measure the recovered watermark robustness. Table .12 summarizes a comparison of the obtained results of BER values under different types of image processing attacks with the proposed DTCWT-DCT and schemes utilized by (Lai, 2011, Makbol et al., 2016 and Ariatmanto et al., 2020).

Table 12. - Comparisons with (Lai, 2011, Mehta et al., 2016 and Ariatmanto et al., 2020) schemes in terms of BER value under various attacks.

Attacks	Lena				Baboon			
	[45]	[6]	[39]	**Proposed scheme**	[45]	[6]	[39]	**Proposed scheme**
No Attack	0,0040	0,0000	**0,0000**	**0,0000**	0,0020	**0,0000**	**0,0000**	0,0332
GF 3x3(1.0)	0,1510	0,0750	**0,0000**	0,0244	0,0840	0,1550	**0,0060**	0,0820
AF 3x3	0,1950	0,2970	**0,0000**	0,0430	0,1190	0,2690	**0,0200**	0,0967
WF 3x3	0,1850	0,2920	**0,0000**	0,0322	0,1200	0,2610	**0,0160**	0,1055
MF 3x3	0,1780	0,0860	**0,0020**	0,0254	0,1450	0,1990	**0,0250**	0,0762
GN001	0,3760	0,0610	**0,0060**	0,0381	0,1960	0,0330	**0,0190**	0,0869
GN005	0,4900	0,1810	0,1180	**0,0410**	0,3790	0,1480	0,1330	**0,0879**
SP001	0,0280	0,0060	0,0110	**0,0000**	0,0210	0,0100	**0,0080**	0,0342
SP005	0,1260	0,0440	0,0420	**0,0010**	0,0990	0,0390	0,0460	**0,0430**
SN005	0,4210	0,0620	0,0480	**0,0029**	0,2190	0,0690	**0,0340**	0,0400
CC50%	0,0330	**0,0040**	0,0240	0,0293	0,2900	0,2220	0,3150	**0,1357**
CO50%	0,2800	0,2670	0,2150	**0,0195**	0,1100	0,1040	**0,0890**	0,0918
CRO50%	0,3390	0,3580	0,2940	**0,0938**	0,1910	0,1530	0,2050	**0,1504**
CCO50%	0,1880	0,1810	0,1160	**0,0771**	0,2670	0,2440	0,2500	**0,1582**
JPEGQ 50	0,2730	0,0310	0,0030	**0,0020**	0,0120	**0,0040**	0,0120	0,0508
JPEGQ 70	0,2700	0,0020	**0,0010**	**0,0010**	0,0030	**0,0020**	0,0060	0,0508

As shown in Table .12; The DTCWT-DCT scheme achieved the lowest BER values of recovered watermark for Lena image against Gaussian noise in the variant of 005, salt and pepper in the density of 0.001 and a density of 0.005, Speckle noise in the density of 0.005, cropping off, in the rate of 50%, cropping row off in the rate of 50%, cropping column off in the rate of 50% and compression JPEG by the quality factor of 50. As regards to Baboon image, lower values were obtained only under Gaussian noise in the variant of 0.005, salt and pepper in the density of 0.005, centred cropping in the rate of 50%, cropping row off in the rate of 50% and cropping column off in the rate of 50%. The scheme proposed by (Ariatmanto et al., 2020) outperformed by the lower BER value under all tested filtered images (average filter (AF), Gaussian filter (GF), wiener filters (WF) and median filters (MF)) for both tested Lena and Baboon images, while the scheme proposed by (Makbol et al., 2016) realized the lowest value of BER compared to other schemes only under centred cropping in the rate 50% Lena image. For more understanding, the comparison of BER values under various image processing attacks between the proposed DTCWT-DCT scheme and the previous schemes proposed by (Lai, 2011, Makbol et al., 2016 and Ariatmanto et al., 2020) were presented in a visual form as shown in Figure .12

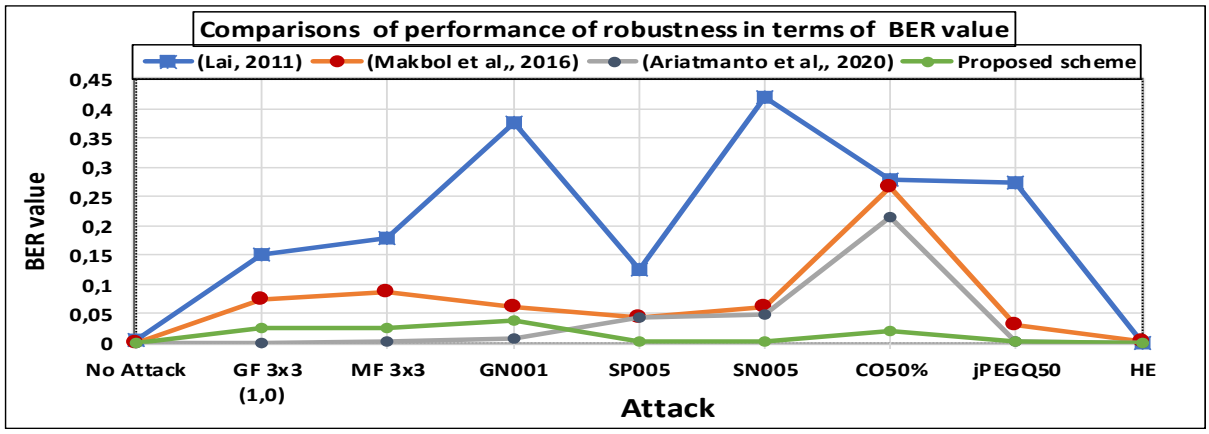

FIGURE 12. - Comparisons with (Lai, 2011, Makbol et al., 2016 and Ariatmanto et al., 2020) schemes in terms of BER value under various attacks

According to Figure .12, the proposed DTCWT-DCT outperformed the schemes proposed by (Lai, 2011, Makbol et al., 2016 and Ariatmanto et al., 2020) in the lowest BER value under the type of image processing attacks salt and pepper in the density of 0.005, Speckle noise in the density of 0.005 and cropping off, in the rate of 50%, except for the scheme proposed by (Ariatmanto et al., 2020) that achieved a lower BER value against the attacks Gaussian filter (MF), median filters (MF) and Gaussian noise in the density of 0.001. However, all proposed schemes succeeded to fully recover the watermark under no attacks and under histogram equalisation (HE) attack as shown in Figure .12.

Another comparison was conducted between the proposed optimization scheme DTCWT-DCT and the related watermarking schemes which used a combination of hybrid domain and the optimization methods under various image processing attacks. Table .13 summarizes the obtained results of the comparison in terms of BER value under various attacks between the proposed scheme DTCWT-DCT and the schemes proposed by Kazemivash et al., (2018) and Kang et al. (2020) as follows:

Table 13. - Comparisons with schemes proposed by Kazemivash et al., (2018) and Kanget al. (2020) schemes in terms of BER value under various attacks.

Attacks	Mandrill			Barbara			Peppers		
	[46]	[21]	**Proposed scheme**	[46]	[21]	**Proposed scheme**	[46]	[21]	**Proposed scheme**
JPEGQ50	0,0273	0,0078	**0,0000**	0.0059	**0,0000**	0,0537	0,0137	**0,0010**	0,0088
JPEGQ75	0,0195	0,0010	**0,0000**	0.0020	**0,0000**	0,0049	0,0020	**0,0000**	**0,0000**
JPEGQ80	0,0068	**0,0000**	**0,0000**	0.0010	**0,0000**	0,0088	0,0010	**0,0000**	**0,0000**
GF(3 x3) (sigma:0,5)	0,0127	0,0049	**0,0000**	**0,0000**	**0,0000**	0,0020	**0,0000**	**0,0000**	**0,0000**
MF(3 x3)	0,0429	0,0010	**0,0000**	0.0068	**0,0039**	0,0332	**0,0010**	0,0029	**0,0010**
AF(3 x 3)	0,0215	0,0068	**0,0000**	**0.0010**	**0,0010**	0,0293	**0,0020**	0,0078	0,0088
WF(3 x 3)	0,0322	0,0039	**0,0000**	0.0020	**0,0000**	0,0381	**0,0000**	0,0029	0,0029
GN005	0,1074	0,1045	**0,0303**	0.0781	0,0706	**0,0381**	0,0811	0,1680	**0,0244**
SP01	0,0557	0,0586	**0,0000**	0.0332	0,0527	**0,0146**	0,0313	0,1025	**0,0010**
SN01	0,0969	0,0781	**0,0000**	0.0352	**0,0000**	0,0088	0,0234	0,0801	**0,0000**
HE	0,0205	0,0029	**0,0000**	0.0010	**0,0000**	**0,0000**	0,0000	0,0010	**0,0000**
SH	0,0088	**0,0000**	**0,0000**	0,0000	**0,0000**	**0,0000**	**0,0000**	**0,0000**	**0,0000**
Cropping (25%)	0,0166	0,1143	**0,0000**	0.0234	0,1143	**0,0049**	0,0039	0,1143	**0,0000**
Resizing (1024 - 2048 - 1024)	**0,0000**	**0,0000**	**0,0000**	**0,0000**	**0,0000**	0,0010	**0,0000**	**0,0000**	**0,0000**
Resizing (1024- 512 -1024)	0,0273	**0,0020**	0,0400	**0,0000**	**0,0000**	0,1309	**0,0000**	0,0010	0,0488

According to Table.13, the proposed optimization scheme DTCWT-DCT mostly outperformed the schemes proposed by Kazemivash et al., (2018) and Kang et al. (2020) in the lowest BER value with image Mandrill under most of the tested image attacks. For both Barbara and Peppers images, the proposed scheme achieved the lowest BER value compared to the other proposed schemes under Gaussian noise in the density of 0.01 and salt and pepper noise in the density of 0.01 while the other proposed schemes attained a lower BER value with Barbara and Peppers images under the image filtering attack and scaling image of 0.5 compared to the proposed scheme DTCWT-DCT.

The results of the lowest BER value indicate that the recovered watermark was nearer to the input watermark. Based on this, it can be said that the proposed DTCWT-DCT scheme significantly succeeded to fully recover the watermark under compression JPEG, Gaussian noise, salt and pepper noise (SP), cropping and histogram equalisation (HE) though distortion appeared on the extracted watermark against the various types of image filtering attack.

The obtained watermarked image and retrieved watermark from the optimization proposed DTCWT-DCT scheme under different image processing attacks will be presented in visual form in the following section.

5.6 THE OBTAINED RESULTS OF THE WATERMARKED IMAGE AND RECOVERED WATERMARK IN VISUAL FORM.

The optimization proposed DTCWT-DCT scheme has proven a robust performance against most kinds of image processing attacks; it was demonstrated through the results' visual quality as shown in Figure.13.

As shown in Figure .13, the optimization proposed DTCWT-DCT scheme demonstrated a better visual quality of the watermarked image besides full recovery of the retrieved watermark against most kinds of attacks except for rotation, gaussian noise and image filtered attacks where distortion appeared on the retrieved watermark.

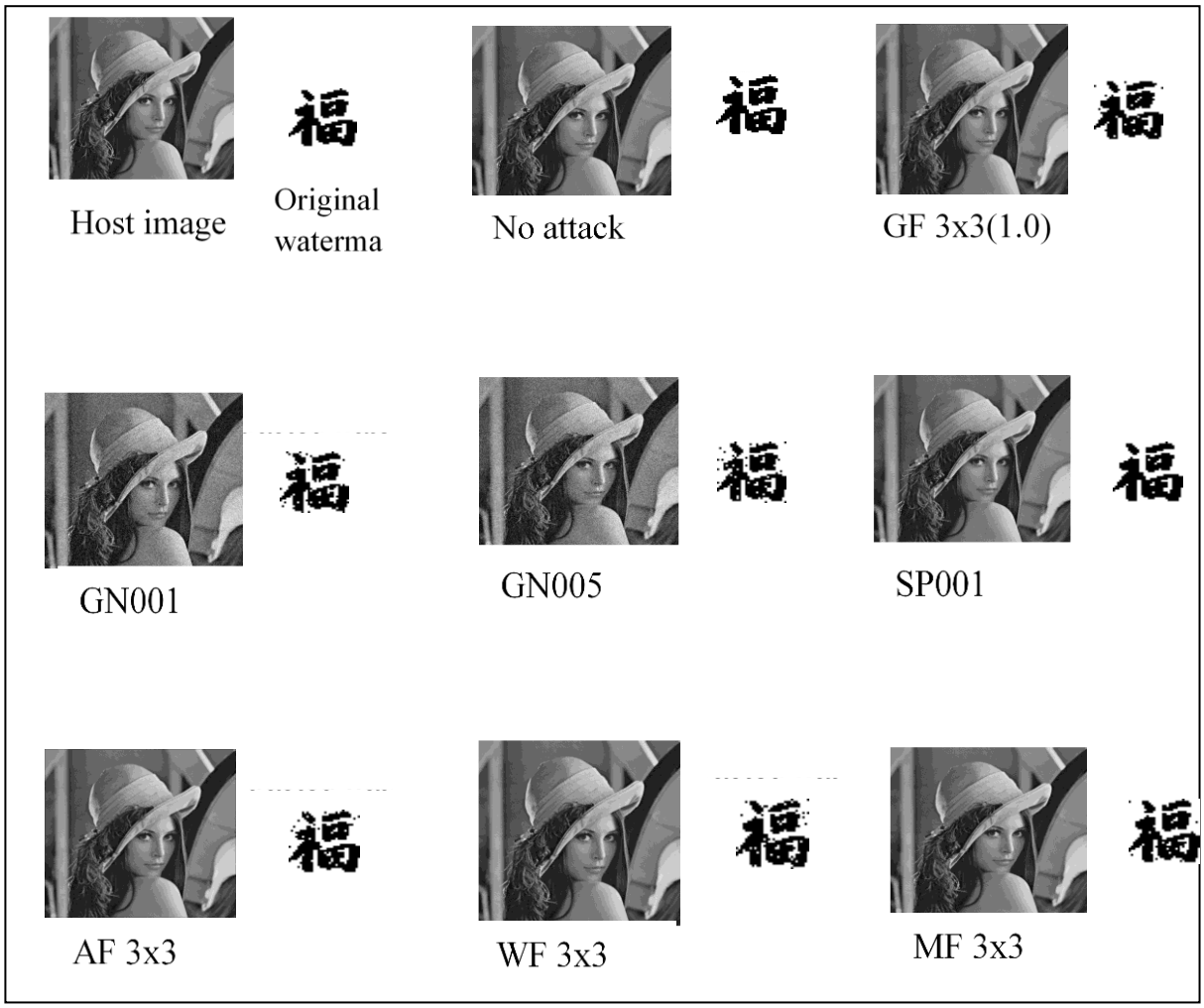

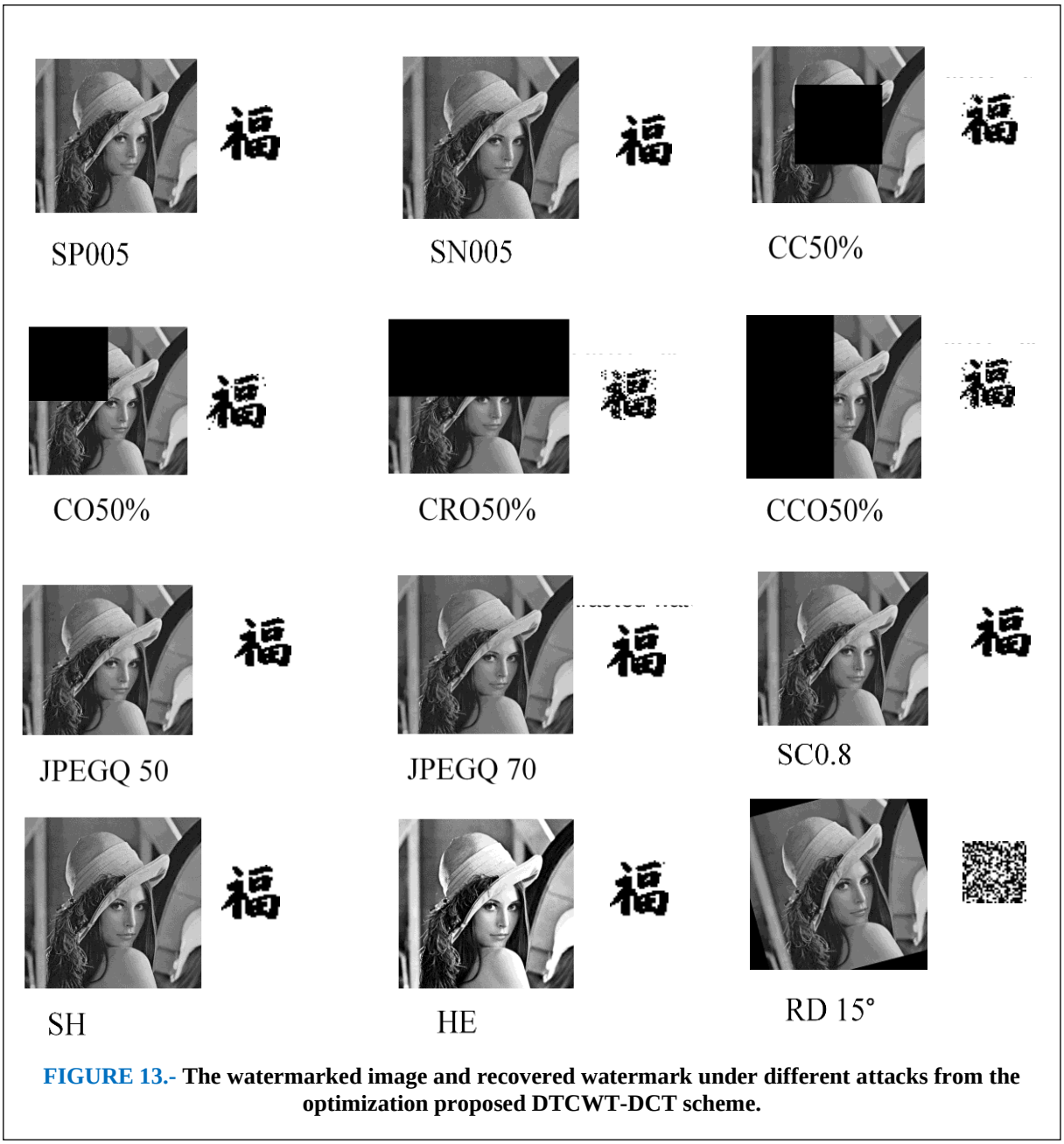

FIGURE 13.- The watermarked image and recovered watermark under different attacks from the optimization proposed DTCWT-DCT scheme.

6. CONCLUSION

The performance of the proposed optimization DTCWT-DCT image watermarking scheme has been evaluated against various types of image processing attacks such as filtered image, noise addition, compression and geometric distortions. Furthermore, it has been compared to previous schemes to prove its performance.

The calculation of an optimal scaling factor based on Secant method during the embedding of the watermark in the transform coefficients generated by combining of the DCT and the DTCWT domains, ensures the strong trade-off between the good imperceptibility and robustness.

The experimental results proved that the proposed optimized DTCWT-DCT scheme outperforms other existing schemes under attacks of cropping and salt & pepper noise. Moreover, it succeeded in fully recover the embedded watermark as shown in terms of NC and BER values without affecting the visual quality of the watermarked image as shown in terms of PSNR values against most tested image attacks. Furthermore, the multitude of sub-bands of the DTCWT decomposition is an additional advantage for improving the security of watermark embedding. Overall, it can be said that the proposed optimized DTCWT-DCT scheme achieved a good trade-off between imperceptibility and robustness against most common image attacks.

As a future work, we suggest the development of a robust and reversible image watermarking scheme based on the findings of this research. As we know, if the scheme is reversible, the original image can be completely recovered, and

the identification step will not suffer from any alteration caused by the watermarking process. Secondly, this research could be developed through using machine learning techniques to optimize and improve the performance of watermarking algorithms. Finally, we suggest the application of the proposed scheme in the domain of video watermarking.

Funding

None

ACKNOWLEDGEMENTS

We would like to show our gratitude to University Malaysia Pahang for supporting this study as part of the research outcome for PhD work.

CONFLICTS OF INTEREST

The author declares no conflict of interest.

REFERENCES

[1] W. Wan, J. Wang, Y. Zhang, J. Li, H. Yu, and J. Sun, “A comprehensive survey on robust image watermarking,” Neurocomputing, 2022.

[2] O. Evsutin and K. Dzhanashia, “Watermarking schemes for digital images: Robustness overview,” Signal Processing: Image Communication, vol. 100, p. 116523, 2022.

[3] T. Huynh-The, O. Banos, S. Lee, Y. Yoon, and T. Le-Tien, “Improving digital image watermarking by means of optimal channel selection,” Expert systems with applications, vol. 62, pp. 177–189, 2016.

[4] D. Ariatmanto and F. Ernawan, “An improved robust image watermarking by using different embedding strengths,” Multimedia Tools and Applications, vol. 79, no. 17, pp. 12041–12067, 2020.

[5] F. Ernawan and M. N. Kabir, “A robust image watermarking technique with an optimal DCT-psychovisual threshold,” IEEE Access, vol. 6, pp. 20464–20480, 2018.

[6] N. M. Makbol, B. E. Khoo, and T. H. Rassem, “Block-based discrete wavelet transform-singular value decomposition image watermarking scheme using human visual system characteristics,” IET Image processing, vol. 10, no. 1, pp. 34–52, 2016.

[7] S. Fazli and M. Moeini, “Optik A robust image watermarking method based on DWT , DCT , and SVD using a new technique for correction of main geometric attacks,” Optik - International Journal for Light and Electron Optics, vol. 127, no. 2, pp. 964–972, 2016.

[8] M. H. Vali, A. Aghagolzadeh, and Y. Baleghi, “Optimized watermarking technique using self-adaptive differential evolution based on redundant discrete wavelet transform and singular value decomposition,” Expert Systems with Applications, vol. 114, pp. 296–312, 2018.

[9] N. Bousnina, S. Ghouzali, M. Mikram, and W. Abdul, “DTCWT-DCT watermarking method for multimodal biometric authentication,” in Proceedings of the 2nd International Conference on Networking, Information Systems & Security, 2019, pp. 1–7.

[10] A. Shaik and V. Masilamani, “A novel digital watermarking scheme using dragonfly optimizer in transform domain,” Computers & Electrical Engineering, vol. 90, p. 106923, 2021.

[11] R. Sihwail, O. S. Solaiman, K. Omar, K. A. Z. Ariffin, M. Alswaitti, and I. Hashim, “A Hybrid Approach for Solving Systems of Nonlinear Equations Using Harris Hawks Optimization and Newton’s Method,” IEEE Access, vol. 9, pp. 95791–95807, 2021.

[12] H. M. Ridha, A. A. Heidari, M. Wang, and H. Chen, “Boosted mutation-based Harris hawks optimizer for parameters identification of single-diode solar cell models,” Energy Conversion and Management, vol. 209, p. 112660, 2020.

[13] O. S. Solaiman, S. A. A. Karim, and I. Hashim, “Optimal fourth-and eighth-order of convergence derivative-free modifications of King’s method,” Journal of King Saud University-Science, vol. 31, no. 4, pp. 1499–1504, 2019.

[14] O. S. Solaiman and I. Hashim, “Optimal eighth-order solver for nonlinear equations with applications in chemical engineering,” Intell. Autom. Soft Comput, vol. 13, pp. 87–93, 2020.

[15] O. S. Solaiman and I. Hashim, “An iterative scheme of arbitrary odd order and its basins of attraction for nonlinear systems,” Comput. Mater. Contin. Computers, vol. 66, pp. 1427–1444, 2021.

[16] K. Zebbiche, F. Khelifi, and K. Loukhaoukha, “Robust additive watermarking in the DTCWT domain based on perceptual masking,” Multimedia Tools and Applications, vol. 77, no. 16, pp. 21281–21304, 2018.

[17] J. Liu et al., “A novel robust watermarking algorithm for encrypted medical image based on DTCWT-DCT and chaotic map,” Computers, Materials & Continua, vol. 61, no. 2, pp. 889–910, 2019.

[18] J. Liu, J. Li, J. Ma, N. Sadiq, U. A. Bhatti, and Y. Ai, “A robust multi-watermarking algorithm for medical images based on DTCWT-DCT and Henon map,” Applied Sciences, vol. 9, no. 4, p. 700, 2019.

[19] J. Liu, J. Ma, J. Li, M. Huang, N. Sadiq, and Y. Ai, “Robust watermarking algorithm for medical volume data in internet of medical things,” IEEE Access, vol. 8, pp. 93939–93961, 2020.

[20] J. Liu, J. Li, K. Zhang, U. A. Bhatti, and Y. Ai, “Zero-watermarking algorithm for medical images based on dual-tree complex wavelet transform and discrete cosine transform,” Journal of Medical Imaging and Health Informatics, vol. 9, no. 1, pp. 188–194, 2019.

[21] X. Kang, Y. Chen, F. Zhao, and G. Lin, “Multi-dimensional particle swarm optimization for robust blind image watermarking using intertwining logistic map and hybrid domain,” Soft Computing, vol. 24, no. 14, pp. 10561–10584, 2020.

[22] F. Thakkar and V. K. Srivastava, “An adaptive, secure and imperceptive image watermarking using swarm intelligence, Arnold transform, SVD and DWT,” Multimedia Tools and Applications, vol. 80, no. 8, pp. 12275–12292, 2021.

[23] \cSeyma Yücel Altay and G. Uluta\cs, “Self-adaptive step firefly algorithm based robust watermarking method in DWT-SVD domain,” Multimedia Tools and Applications, vol. 80, no. 15, pp. 23457–23484, 2021.

[24] A. M. Abdulazeez, D. M. Hajy, D. Q. Zeebaree, and D. A. Zebari, “Robust watermarking scheme based LWT and SVD using artificial bee colony optimization,” Indonesian Journal of Electrical Engineering and Computer Science, vol. 21, no. 2, pp. 1218–1229, 2021.

[25] K. Swaraja, K. Meenakshi, and P. Kora, “An optimized blind dual medical image watermarking framework for tamper localization and content authentication in secured telemedicine,” Biomedical Signal Processing and Control, vol. 55, p. 101665, 2020.

[26] E. Hatami, H. Rashidy Kanan, K. Layeghi, and A. Harounabadi, “An optimized robust and invisible digital image watermarking scheme in Contourlet domain for protecting rightful ownership,” Multimedia Tools and Applications, pp. 1–31, 2022.

[27] A. M. Abdelhakim and M. Abdelhakim, “A time-efficient optimization for robust image watermarking using machine learning,” Expert Systems with Applications, vol. 100, pp. 197–210, 2018.

[28] I. A. Ansari and M. Pant, “Quality assured and optimized image watermarking using artificial bee colony,” International Journal of System Assurance Engineering and Management, vol. 9, no. 1, pp. 274–286, 2018.

[29] A. Mohan, A. Anand, A. K. Singh, R. Dwivedi, and B. Kumar, “Selective encryption and optimization based watermarking for robust transmission of landslide images,” Computers and Electrical Engineering, vol. 95, p. 107385, 2021.

[30] A. Pourhadi and H. Mahdavi-Nasab, “A robust digital image watermarking scheme based on bat algorithm optimization and SURF detector in SWT domain,” Multimedia Tools and Applications, pp. 1–25, 2020.

[31] V. Sharma and R. N. Mir, “An enhanced time efficient technique for image watermarking using ant colony optimization and light gradient boosting algorithm,” Journal of King Saud University-Computer and Information Sciences, 2019.

[32] K. Soppari and N. S. Chandra, “Development of improved whale optimization-based FCM clustering for image watermarking,” Computer Science Review, vol. 37, p. 100287, 2020.

[33] S. M. Almufti, A. A. Shaban, Z. A. Ali, R. I. Ali, and J. A. Dela Fuente, “Overview of Metaheuristic Algorithms,” Polaris Global Journal of Scholarly Research and Trends, vol. 2, no. 2, pp. 10–32, 2023.

[34] A. H. Halim, I. Ismail, and S. Das, Performance assessment of the metaheuristic optimization algorithms: an exhaustive review, vol. 54, no. 3. Springer Netherlands, 2021.

[35] P. Singh, A. Singhal, and S. D. Joshi, “An efficient ML frequency estimation of a sinusoid using the Secant method,” 11th IEEE International Conference on Advanced Networks and Telecommunications Systems, ANTS 2017, pp. 1–5, 2018.

[36] K. Ramani, E. V. Prasad, and S. Varadarajan, “Protecting Digital Images Using DTCWT-DCT,” in Communications in Computer and Information Science, 2010, vol. 101, pp. 36–44.

[37] K. H. A. Sahid, V. Thomas, S. Kumaravel, and S. Ashok, “Performance comparison of root-finding algorithms for solar photovoltaic emulator,” 1st International Conference on Power Electronics Applications and Technology in Present Energy Scenario, PETPES 2019 - Proceedings, pp. 1–5, 2019.

[38] J. Cai, M. Martorella, S. Chang, Q. Liu, Z. Ding, and T. Long, “Efficient Nonparametric ISAR Autofocus Algorithm Based on Contrast Maximization and Newton’s Method,” IEEE Sensors Journal, vol. 21, no. 4, pp. 4474–4487, 2021.

[39] D. Ariatmanto and F. Ernawan, “Adaptive scaling factors based on the impact of selected DCT coefficients for image watermarking,” Journal of King Saud University-Computer and Information Sciences, 2020.

[40] W.-L. Lyu, C.-C. Chang, T.-S. Nguyen, and C.-C. Lin, “Image watermarking scheme based on scale-invariant feature transform,” KSII Transactions on Internet and Information Systems (TIIS), vol. 8, no. 10, pp. 3591–3606, 2014.

[41] T. Tagesse Takore, P. Rajesh Kumar, and G. Lavanya Devi, “A robust and oblivious grayscale image watermarking scheme based on edge detection, SVD, and GA,” in Proceedings of 2nd International Conference on Micro-Electronics, Electromagnetics and Telecommunications, 2018, pp. 51–61.

[42] R. Mehta, N. Rajpal, and V. P. Vishwakarma, “Adaptive image watermarking scheme using fuzzy entropy and GA-ELM hybridization in DCT domain for copyright protection,” Journal of Signal Processing Systems, vol. 84, no. 2, pp. 265–281, 2016.

[43] C. Agarwal, A. Mishra, and A. Sharma, “Gray-scale image watermarking using GA-BPN hybrid network,” Journal of Visual Communication and Image Representation, vol. 24, no. 7, pp. 1135–1146, 2013.

[44] J. Han, X. Zhao, and C. Qiu, “A digital image watermarking method based on host image analysis and genetic algorithm,” Journal of Ambient Intelligence and Humanized Computing, vol. 7, pp. 37–45, 2016.

[45] C.-C. Lai, “An improved SVD-based watermarking scheme using human visual characteristics,” Optics Communications, vol. 284, no. 4, pp. 938–944, 2011.

[46] B. Kazemivash and M. E. Moghaddam, “A predictive model-based image watermarking scheme using regression tree and firefly algorithm,” Soft Computing, vol. 22, pp. 4083–4098, 2018.